Distribution Agreement

In presenting this thesis or dissertation as a partial fulfillment of the requirements for an advanced degree from Emory University, I hereby grant to Emory University and its agents the non-exclusive license to archive, make accessible, and display my thesis or dissertation in whole or in part in all forms of media, now or hereafter known, including display on the world wide web. I understand that I may select some access restrictions as part of the online submission of this thesis or dissertation. I retain all ownership rights to the copyright of the thesis or dissertation. I also retain the right to use in future works (such as articles or books) all or part of this thesis or dissertation.

Signature:

_____	_____
Seonhee Kong	May 1, 2021

Identifying and Analyzing Nonlinear Concentration-Response Relationships in Tox21 Thyroid Receptor Assays

By

Seonhee Kong
Master of Public Health

Gangarosa Department of Environmental Health

Qiang Zhang, MD, PhD
Committee Chair

Identifying and Analyzing Nonlinear Concentration-Response Relationships in Tox21 Thyroid Receptor Assays

By

Seonhee Kong

B.S.N.
Korea Armed Forces Nursing Academy
2012

Thesis Committee Chair: Qiang Zhang, MD, PhD

An abstract of
a thesis submitted to the Faculty of the
Rollins School of Public Health of Emory University
in partial fulfillment of the requirements for the degree of
Master of Public Health
in Environmental Health
2021

Abstract

Identifying and Analyzing Nonlinear Concentration-Response Relationships in Tox21 Thyroid Receptor Assays

By Seonhee Kong

Background: Environmental thyroid disrupting chemicals (TDCs) can exhibit nonlinear including nonmonotonic dose response (NMDR) behaviors at low doses. NMDR presents a serious challenge because it could be difficult to accurately predict the risk of exposure to a particular chemical. New risk assessment methodologies produce toxicity testing results that are efficient and suitable for human application via *in vitro* assays. This study was aimed to analyze the concentration-response curves and identify nonlinearities including NMDR in the Tox21 high-throughput screening (HTS) data of thyroid receptor (TR) assays.

Methods: The Tox21 quantitative HTS TR assay data from the National Center for Advancing Translational Sciences (NCATS) were used. For the TR assays conducted in the antagonist or agonist mode and the viability assay, 10,496 chemicals (10K) were screened each. Among averaged concentration-response curves, the curves which have either low variance levels or response levels bound in a certain range were screened out. Correlation-based algorithm was applied for clustering followed by supervised learning algorithm for curve classification into five shapes – U, Bell, monotonic increasing, monotonic decreasing, and flat. Additional filtering was done based on viability and interference assays. For those remaining monotonic increasing or decreasing curves, their Hill coefficients were assessed for degree of nonlinearities.

Results: After all the screenings, 1,353 monotonic decreasing curves, 263 monotonic increasing curves, 577 U curves, 88 Bell curves were identified in antagonist mode assays. 16 monotonic decreasing curves, 19 monotonic increasing curves, 1 U curve, 9 Bell curves were identified in agonist mode assays. In antagonist mode assays, among known TDCs, TBBPA, pentachlorophenol, triclosan, and BPA exhibit as monotonic decreasing shapes, some of which have Hill coefficients considerably greater than 1 representing high degree of nonlinearities. Methimazole, propylthiouracil were classified as U shape.

Conclusions: The Tox21 TR assays contain many concentration-response curves that are either nonmonotonic or highly nonlinear even though they are monotonic, suggesting nonlinear dose response of endocrine disruptors can arise at the gene transcription level. Identifying nonlinear concentration-response relationship and underlying mechanisms will help provide a scientific basis for improving safety assessment of chemical products.

Identifying and Analyzing Nonlinear Concentration-Response Relationships in Tox21 Thyroid Receptor Assays

By

Seonhee Kong

B.S.N., Korea Armed Forces Nursing Academy, 2012

Thesis Committee Chair: Qiang Zhang, MD, PhD

A thesis submitted to the Faculty of the
Rollins School of Public Health of Emory University
in partial fulfillment of the requirements for the degree of
Master of Public Health
in Environmental Health
2021

Acknowledgements

I would like to begin by expressing gratitude to all personnel from my home country, the Republic of Korea, who are working day and night to prevent further loss of life under the COVID-19 pandemic. Being a military nursing officer, I am especially grateful to the efforts of my country's military and Nursing Corps. I pray that all our efforts bring an end to this pandemic at the earliest.

I am deeply grateful to my academic advisor, Professor Qiang Zhang in the Gangarosa Department of Environmental Health, for his interest and consideration for my work. Our weekly meetings during my course guided me through my thesis and other new experiences in graduate school. Without him, I wouldn't have been able to reach this stage in my graduate degree.

I am grateful to Youmi Kim, my fellow student and friend, who empathized with my difficulties more than anyone else and was most helpful in navigating them. She was very supportive through my transition to living in a foreign country for the first time.

I am also grateful to Ye-jin, my life-long mentor, whom I met as a young cadet at the age of 20. I was curious about the world in general and Ye-jin was my partner in exploring many things together.

I am thankful to Bo-ram, who is on the same professional path as I am, except in Korea. My conversations with her have helped me endure the difficulties of living abroad with hope of returning to my country in the future.

I would like to express my gratitude to William, my colleague from the military who was always ready with messages of encouragement whenever I faced a difficult moment. To this end, I am grateful to the support of my high school friends, Cho-yeon and In-hwa, who can cheer me up even without words.

Last but not the least, I extend endless gratitude to my parents for silently cheering me on as I choose one difficult path after another. As I fulfill my duties as a soldier, I am grateful to my younger brother Seong-hwan, who is always by my parents' side on my behalf when I cannot be.

Looking back on my two years in Atlanta, United States, I cannot say that they have been easy, but they have taught me a lot about my inner strength. I will carry my invaluable experiences in this city as I return to being a military nursing officer who can contribute to medical care in the Republic of Korea.

Table of Contents

1. Introduction

1.1. Thyroid system in general

One of the most concerning public health issues is the interference with the normal metabolism and actions of endogenous hormones by environmental endocrine disrupting chemicals (EDCs). While the greatest focus has been on the potential interactions of chemicals with the sex steroid hormone system, there have been numerous lines of evidence that these EDCs affect the thyroid hormone (TH) system as well (Ghisari and Bonefeld-Jorgensen 2005).

The concentrations of THs in the plasma and tissues are elaborately regulated by the control of a feedback system which consists of the hypothalamus, anterior pituitary, and thyroid gland (HPT axis) (Yen 2001). Each tissue/gland of the HPT system secretes specific hormones. In the hypothalamus, thyrotropin-releasing hormone (TRH) is synthesized in the paraventricular nuclei (PVN) (Zoeller, Tan et al. 2007, Fliers, Kalsbeek et al. 2014). TRH is transported to the anterior pituitary and binds to the TRH receptor (TRHR) to stimulate the synthesis and secretion of thyroid-stimulating hormone (TSH) (Zoeller, Tan et al. 2007). TSH binds to its G protein coupled receptors on the thyrocytes in the follicles of the thyroid gland. TSH then promotes iodine uptake and the synthesis and secretion of THs, including triiodothyronine (T_3) and thyroxine (T_4), to the systemic circulation (Zoeller, Tan et al. 2007). Thyroid specific genes, including Na^+/I^- symporter (NIS), thyroglobulin (TG), and thyroid peroxidase (TPO), are involved and regulated by TSH in these processes (Yen 2001).

THs play a crucial role in growth, development and energy homeostasis (Silva 2001). THs influence a number of biological processes in the body and are essential for regulating metabolism, bone remodeling, cardiac function and mental status (Boas, Feldt-Rasmussen et al. 2012).

1.2. Disruption of the thyroid system by environmental chemicals

1.2.1. Thyroid Disruptors and Mechanisms

Recent epidemiological and toxicological studies have shown that numerous contaminants can reduce circulating TH levels and thus disrupt TH signaling in the body (Boas, Feldt-Rasmussen et al. 2006). According to the National Institutes of Health (NIH) definition, the thyroid-disrupting chemicals (TDCs) refer to xenobiotics that interfere with TH signaling (Miller, Crofton et al. 2009). Given the diversity and complexity of the mechanisms involved in thyroid homeostasis, TDCs have vastly different actions at different levels of the thyroid system. These biological actions include the following; altering the structure or function of the thyroid gland itself (e.g., perchlorate and methimazole), altering binding of hormones to thyroid receptors (e.g., bisphenol A (BPA), polychlorinated biphenyls (PCBs), polybrominated diphenyl ethers (PBDEs), or altering regulatory enzymes involved in TH synthesis (e.g., propylthiouracil (PTU)) (Crofton and Zoeller 2005, Miller, Crofton et al. 2009). Aside from thyroidal mechanisms, a large number of extrathyroidal mechanisms affect circulating TH levels by altering binding to hormone transport proteins (e.g., hydroxyl-PCBs, EMD 49209 and pentachlorophenol), hepatic clearance (e.g., PCBs and triclosan), and inhibition of deiodination of T_4 to T_3 (e.g., FD&C red dye number 3, PTU, PCBs, octylmethoxycinnamate) (Miller, Crofton et al. 2009).

1.2.2. General Health Outcome of TDCs

Although noticeable changes in hormone levels in animals and in the human body due to small amounts of TDCs existing in the environment are difficult to observe, it is clear that they adversely affect hormonal homeostasis (Boas, Feldt-Rasmussen et al. 2006). Exposure to PCBs, one of the well-known TDCs, had an inverse association with T_3 in men (Meeker, Altshul et al. 2007). In addition, there is a growing concern that TDCs may increase cardiovascular risk

in humans by reducing serum T_4 (Boas, Feldt-Rasmussen et al. 2012). Because THs regulate a number of genes involved in the developing brain, it's not difficult to infer that TH disruption can adversely affect the brain maturation process (Bernal 2005, Ghisari and Bonefeld-Jorgensen 2009). Neurological deficits and irreversible mental retardation may occur due to altered TH levels caused by TDC exposure during the fetal and postnatal periods when the central nervous system is developing and maturing (Howdeshell 2002, Morreale de Escobar, Obregon et al. 2004). While not much has been established about the effects of THs on sexual development, it is known that hypothyroidism and hyperthyroidism affect sexual development in both males and females, especially during puberty (Cargnelutti, Di Nisio et al. 2020). TH imbalances, which originate from hypothyroidism and hyperthyroidism, disturb the metabolic pathways of the body and have a profound effect on metabolic diseases such as obesity and diabetes (Schug, Janesick et al. 2011, Medici, Visser et al. 2015).

1.2.3. Nonlinear Dose-Response of TDCs

EDCs including TDCs can exhibit nonlinear, including nonmonotonic, dose response (NMDR) behaviors at low doses (Vandenberg, Colborn et al. 2012). The U.S. Environmental Protection Agency (EPA) defines NMDRs as measured biologic effects with dose response curves that contain a point of inflection where the slope of the curve changes sign at one or more points within the tested range. They are of particular concern in the context of chemical toxicity testing and risk assessments as they do not follow the generally expected linear or threshold dose response that would be monotonously increasing or decreasing in activity followed by increasing dose (Zoeller, Tan et al. 2007, Vandenberg, Colborn et al. 2012).

NMDRs generally take the form of either a decrease in the response at low dose followed by an increase at high dose (called a U-shape in this study), or vice versa (a Bell-

shape in this study). NMDR presents a serious challenge because it could be difficult to accurately predict the risk of exposure to a particular chemical by using the traditional concepts of LOAEL (lowest observed adverse effect level) or NOAEL (no observed adverse effect level) (Vandenberg, Colborn et al. 2012, Klimenko 2021).

It is well known that exposure to high concentrations of EDCs affects the reproductive system, nervous system, metabolic system, and immune system through toxicity. However, it is worrisome when exposure to even low concentrations may have similar health effects through endocrine disturbance. The characteristics of these endocrine disruptors show unexpected reactivity at low concentrations that are considered to be below the safety standard, but do not show reactivity when the concentration increases. This suggests the possibility that low exposure to many chemicals that we currently believe are safe may not be safe.

1.2.4. Toxicity Testing of Thyroid Disruptors

Currently, most risk assessment strategies rely on chemical toxicity data obtained from animal testing. This conventional animal testing is expensive, slow and inefficient, and may be inadequate to recapitulate results for human health outcomes. In addition, this approach to toxicity testing can pose animal right issues (Freitas, Miller et al. 2014). Due to the complex nature of EDCs, there is a skeptical view that it is difficult to properly evaluate the health effects of EDCs with the traditional testing techniques in use.

Movements, which stems from the need for animal-alternative testing with more reliable results, including *in vitro* methods, are gradually gaining traction and expanding their scope. The U.S. EPA initiated NexGen project to devise the next generation of risk science (Cote, Anastas et al. 2012). "Toxicity Testing in the 21st Century (TT21C): A Vision and a

Strategy" (NRC 2007), a report also referred to as a major keystone of the NexGen framework, was published in 2007 by the Committee on Toxicity Testing and Assessment of Environmental Agents of the National Research Council (Krewski, Westphal et al. 2014). New risk assessment methodologies, including the new approach methodology (NAM), have a common foothold to produce toxicity testing results that are more efficient, low-cost, and more suitable for human application by using human cells or organoids via *in vitro* assays.

There have been national efforts to develop screening methods using *in vitro* assays. The endocrine disruptor screening program (EDSP) was set up to screen environmental chemicals in a tiered testing system (Miller, McMullen et al. 2017). The Toxicity Forecaster (ToxCast) and Tox21 programs organize high-content cellular assays using high-throughput screening (HTS) technologies for rigorous toxicologic evaluation and a better understanding of the mechanisms of biomolecular action that have not yet been identified (Ghisari and Bonefeld-Jorgensen 2005, Zhang, Li et al. 2018). The ToxCast program tested hundreds of chemicals and prioritized the toxicity testing of environmental chemicals (Dix, Houck et al. 2007, Miller, McMullen et al. 2017). A U.S. federal interagency collaboration, known as Tox21, involves the National Institute of Environmental Health Sciences (NIEHS)/National Toxicology Program (NTP), the EPA's National Center for Computational Toxicology, the U.S. Food and Drug Agency (FDA), and the National Center for Advancing Translational Sciences (NCATS). An outmost effort of the U.S. Tox21 program is profiling a 10K-compound library against a panel of stress-related and nuclear receptor signaling pathway assays using qHTS approach (Hsieh, Sedykh et al. 2015). The collaborative research has been testing the 10K chemical library in about 70 qHTS assays since Tox21's inception in 2008.

1.2.5. Purpose of This Study

This study was aimed to analyze the concentration-response curves in the Tox21 HTS data of thyroid receptor assays and identify nonlinearities including NMDR.

2. Methods

2.1. Tox21 TR assays

For the Tox21 TR assays, the GH3 (rat pituitary tumor) TRE.Luc reporter gene system was used. The GH3 cells stably hosts a TR, TRα (NR1A1) and TRβ (NR1A2), activity sensor consisting of TH response elements (TRE), which drive the expression of a luciferase reporter gene (Grimaldi, Boulahtouf et al. 2015). Figure 1 illustrates the schematic of the TR-dependent reporter gene expression: (1) THs or a xenobiotics, X, are up-taken into the cells. (2) X binds to the TR and then form a heterodimer with retinoid X receptor (RXR). Homodimers of TR have also been reported (Freitas 2012). (3) Coactivators are recruited to the dimer complex bound to TRE, followed by (4) the expression of the reporter gene (luciferase) which generates a detectable luminescent signal after the substrate is added.

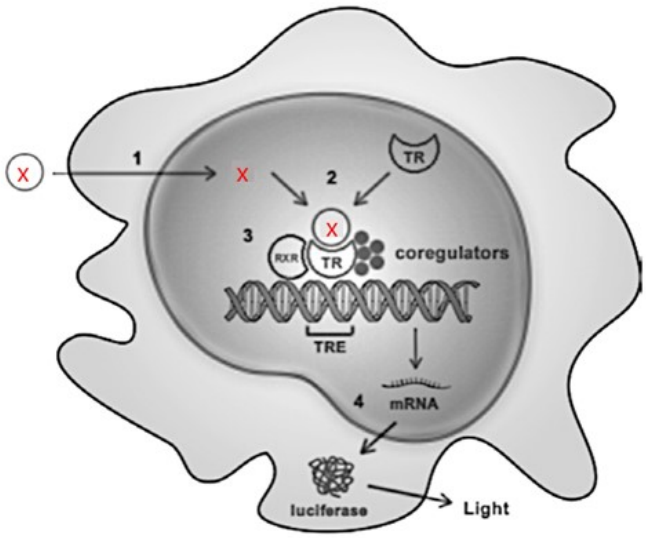

Figure 1. Illustration of mechanism of action of a thyroid hormone receptor-dependent reporter gene cell line. Adapted from Freitas (2012)

We obtained the Tox21 qHTS TR assay data from the National Center for Advancing Translational Sciences (NCATS) Tox21 browser (https:// tripod.nih.gov/tox21/assays/). The relevant qHTS assays include: (1) qHTS assay to identify small molecule antagonists of the

thyroid receptor (TR) signaling pathway, (2) qHTS assay to identify small molecule antagonists of the thyroid receptor (TR) signaling pathway – cell viability counter screen, (3) qHTS assay to identify small molecule agonists of the thyroid receptor (TR) signaling pathway, and (4) qHTS assay to identify small molecule inhibitors of firefly luciferase.

The Tox21 chemical library was screened in triplicate or higher number of replicates (up to 45 replicates in TR assays) for concentration-response, with concurrent cytotoxicity measurements. The distributions of replicates in the TR assays in the antagonist and agonist modes are presented in Figure 2. Each row in the downloaded dataset corresponds to one replicate for one chemical, and contains 15 data points representing the assay responses to 15 concentrations of the screened chemicals. For the TR assays conducted in the antagonist or agonist mode and the viability assay, 10,496 chemicals (10K) were screened each. There are 9,667 chemicals in the interference assay data, among which 7,037 overlap with the TR assay and viability data.

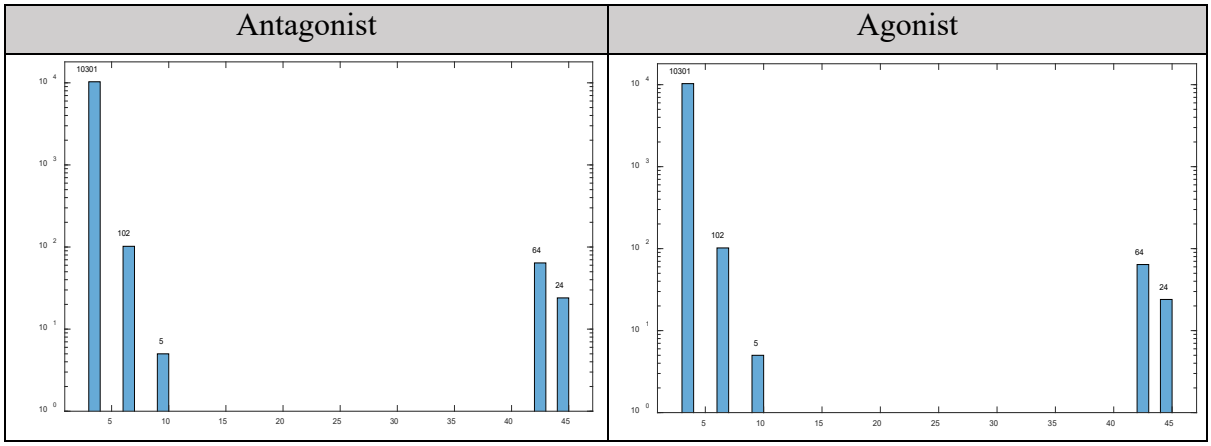

Figure 2. Distribution of replicates in TR antagonist and agonist assays.

2.2. Methods for clustering and classification of dose-response curves

2.2.1. Quality Control

An average concentration-response curve over replicates (3 to 45) was obtained for each chemical in each assay. The curves which have either i) low variance or ii) response levels bound in a certain range were regarded as no or low activities and were screened out. The thresholds used for variance and response screening were specified depending on the distributions of variances, maximal and minimal response values (Figures 3 and 4). If a curve in the antagonist or agonist assay has a response point at a concentration greater than 40 compared to its two immediate neighboring concentrations, the curve was filtered out since it is likely to be outlier and will be examined separately.

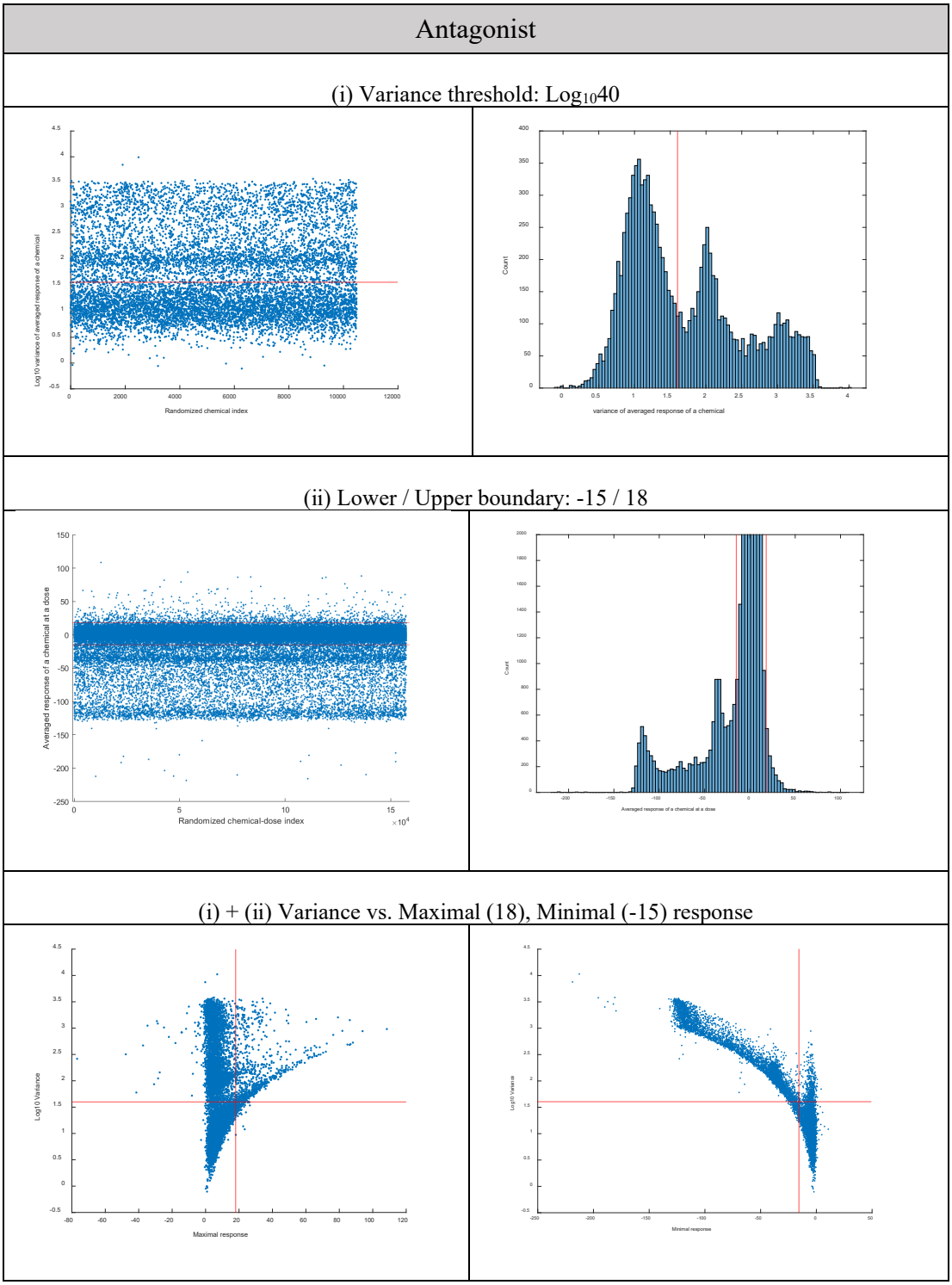

Figure 3. Distributions of variances, all response values, maximal and minimal response values in the antagonist mode

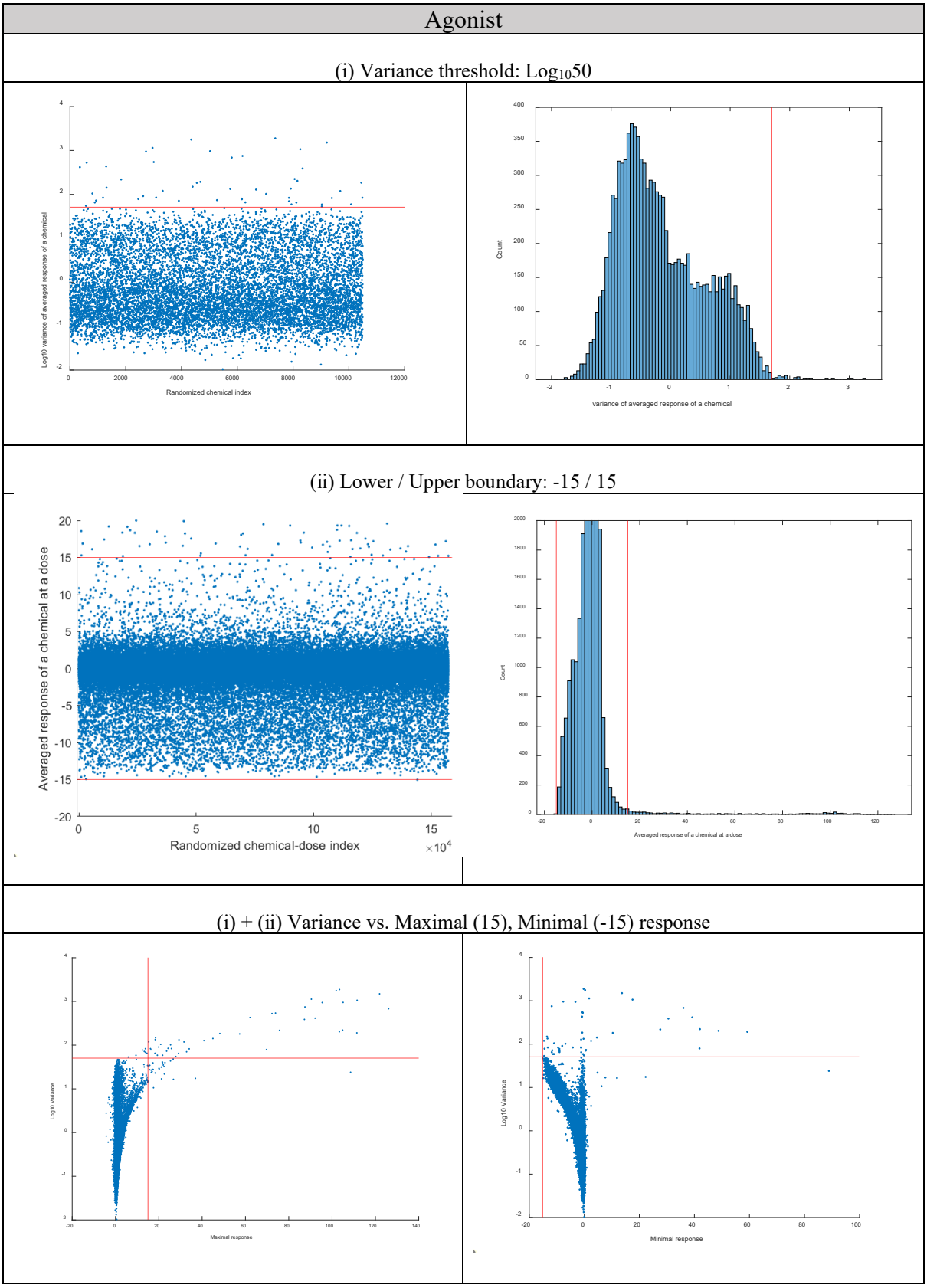

Figure 4. Distributions of variances, all response values, maximal and minimal response values in the agonist mode

2.2.2. Unsupervised Learning Algorithm (Clustering)

The following MATLAB correlation-based algorithm was applied for clustering according to Figure 5. The moving-average (MA) of each chemical's average concentration-response curve was calculated to reduce the local effect of variation. Each cluster was created when the correlation coefficient between the curves is greater than 0.75.

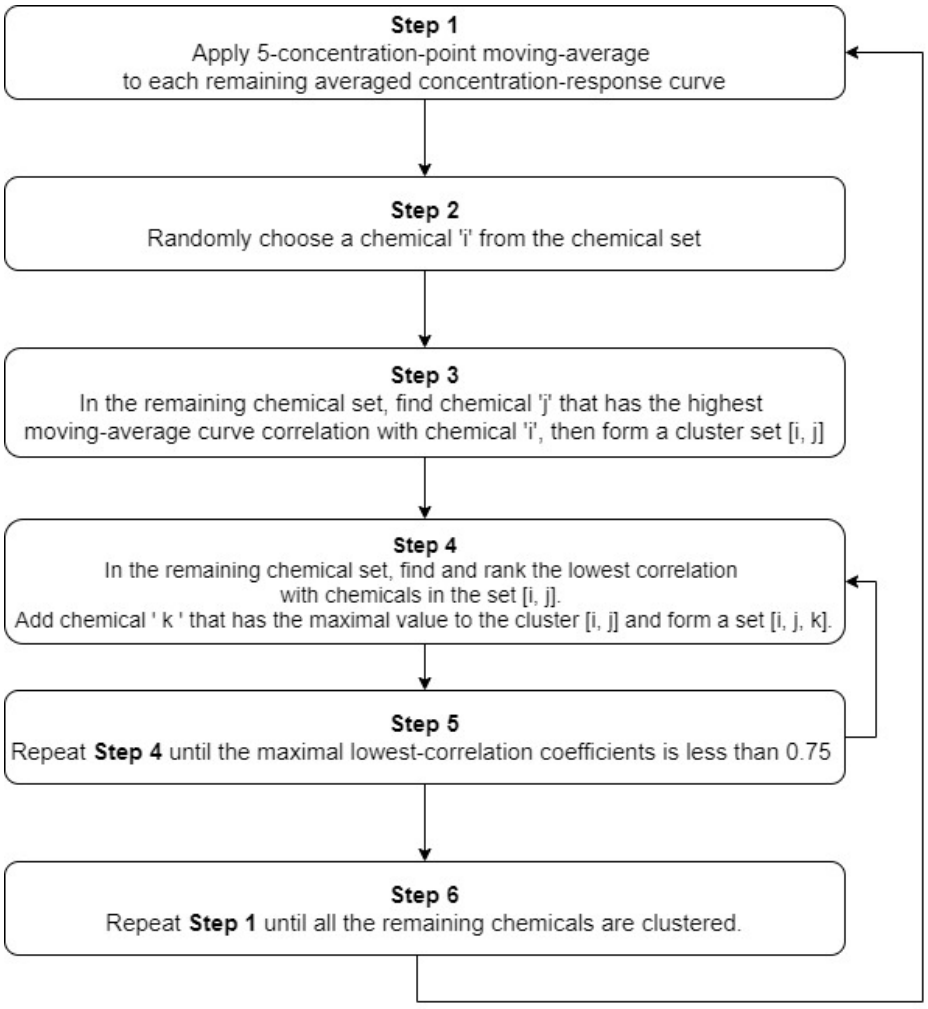

Figure 5. Unsupervised Learning Algorithm adapted from Shi, Xia et al. (2020)

2.2.3. Supervised Learning Algorithm (Curve Classification)

Based on the results from the unsupervised learning algorithm, the clusters were consolidated into five shapes - U, Bell, monotonic increasing, monotonic decreasing, and flat. To better allocate each curve into each of the five shapes, a supervised, classification algorithm was applied (Figure 6). At first, MA using five concentration points was applied to classify Bell, U, and other shapes by using specific magnitude values, and minimal/maximal response levels. The non NMDR curves (other shapes) then were further classified by applying moving average using two concentration points to detect for NMDR curves that were missed out by using MA=5. These were further classified into Bell, U, flat, monotonic increasing and decreasing shapes by using the same magnitude values, and minimal/maximal response levels as above.

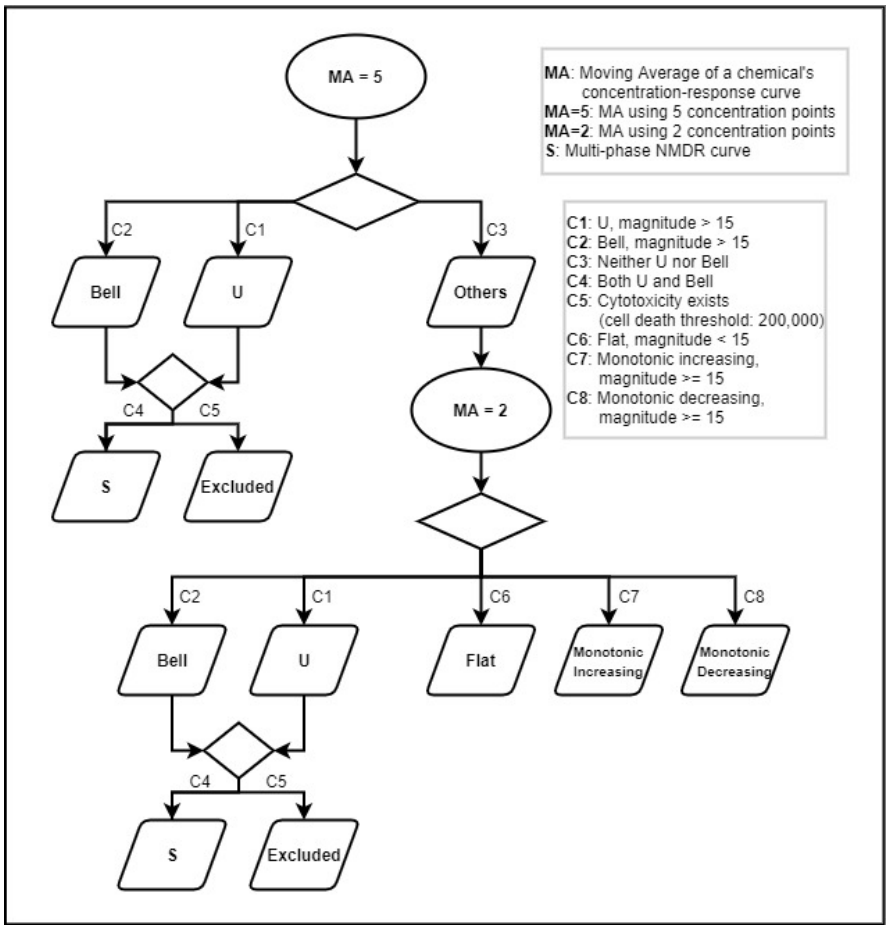

Figure 6. Supervised Learning Algorithm adapted from Shi, Xia et al. (2020)

2.2.4. Additional Filtering Based on Viability and Interference Assays

After the processes of clustering and classification, we tried to filter out those average concentration-response curves that are likely caused by cytotoxicity and interference due to inhibition of luciferase by the tested chemical. In the same manner as in the quality control step above, curve falling within the cut-offs corresponding to the criteria shown in Figure 7 in the viability and interference assays were regarded as no or low activities, and were discarded.

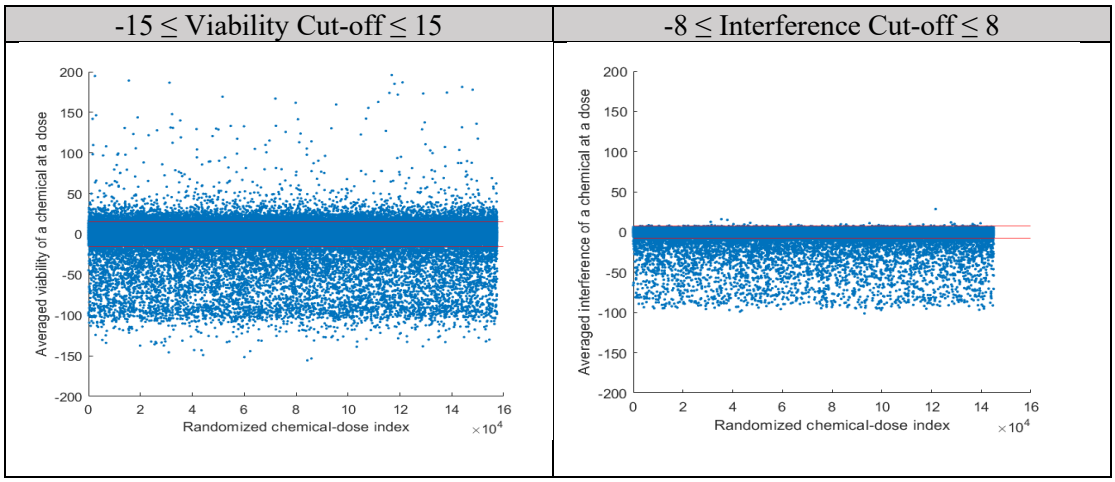

Figure 7. Distributions of averaged responses in viability and interference assays

Afterward, for each of the remaining cytotoxicity curve, we first found the concentration point at which the viability decreases by > 12 from the previous lower concentration point. We then examined the next two lower concentrations. If the viabilities increased by > 5, then the lower concentration will be used as the starting concentration point of cytotoxicity. If the trends of the agonist or antagonist activity curve and the viability curve after the starting concentration point were highly correlated (evaluated by Pearson correlation coefficient > 0.5 and P value <0.2), it was judged that the activity was due to cytotoxicity and the response curve will be filtered out. The above filtering was applied to monotonic decreasing / Bell shapes. The reason we set the cut-offs to be stringent is to filter out as many disqualified curves as possible to retain only true monotonic decreasing or Bell shaped curves. An increasing trend in viability was applied to monotonic increasing / U shapes.

We also conducted the interference screening in a similar logic as the above. Correlation between the two curves was examined only when the chemical was included in the interference assay (only 7,037 of the 10,496 chemicals had interference data). We first found the concentration point at which the luminescence signal decreases by > 8. We then examined the next two lower concentrations. If the signal increased by > 3, then the lower concentration will be used as the starting concentration point of luminescence interference. A similar correlation step was followed as for the viability assay.

2.2.5. Hill Function to Assess Nonlinearities in Monotonic Curves

For those monotonic increasing or decreasing curves, their Hill coefficients were assessed for degree of nonlinearities. The fitted curve for the 15 concentration-response points were obtained using the MATLAB function, 'Fit option'. The initial values of 'AC50 (K)', 'Hill Coefficient (n)', 'Infinite-Activity (y_max)', and 'Zero-Activity (y_min)' were obtained by using the averaged values provided in the Tox21 dataset. The following boundary conditions were used: 6E-10<K<2E-4, -20<n<20, -25<y_max<250, -250<y_min<25. In addition, we compared the Hill coefficient value obtained through the fitted curve with the Hill coefficient value provided in the Tox21 dataset.

3. Results

3.1. Antagonist Assay

3.1.1. Statistics of Concentration-Response Curves in Each Shape

After the initial screening using the variance and boundary criteria above, 5,393 chemicals were filtered out, and 5,103 (48.62%) chemicals remained (Figure 8). Additional 162 chemicals were filtered through the second outlier peak screening criterion, and 4,941 (47.08%) chemicals remained.

As a result of applying the unsupervised algorithm, when the correlation of the chemical dose-response curves is 0.75 or higher, a total of 80 different clusters were obtained. These clusters were visually inspected and consolidated into 6 shape categories: flat, monotonic decreasing, monotonic increasing, U, Bell, and S curves. After applying the supervised algorithm, these curves were classified into 1,020 flat curves (9.72%), 2,749 monotonic decreasing curves (26.19%), 326 monotonic increasing curves (3.05%), 608 U curves (5.79%), 220 Bell curves (2.10%), and 18 S curves (0.17%) (Figure 8).

Two additional screenings were conducted within the categories of monotonic shapes (decreasing and increasing) and non-monotonic shapes (U and Bell) based on the viability and interference data. In the first screening, those with low cytotoxicity (viability -15~15) and low luminescence interference (-8~8) were retained. As a result, 1,182 (11.26%) curves were retained from the previous decreasing shape, 211 (1.95%) from the previous increasing shape, 386 (3.67%) from the previous U shape, and 79 (0.76%) from the previous Bell shape.

In the second screening process, the exclusion criteria were set by the degree of correlation. Those with a correlation coefficient of greater than 0.5 and a p-value of 0.20 or

less between the viability and activity curves on the segment of significant cytotoxicity or interference as detailed in Methods were excluded. As a result, 1,396 were excluded from the previous decreasing shape, leaving 1,353 (12.89%), 63 excluded from the previous increasing shape, leaving 263 (2.45%), 31 excluded from the previous U shape, leaving 577 (5.49%), and 132 excluded from the previous Bell shape, leaving 88 (0.85%). The whole process described above, screening standards and results, are schematically shown in Figure 8.

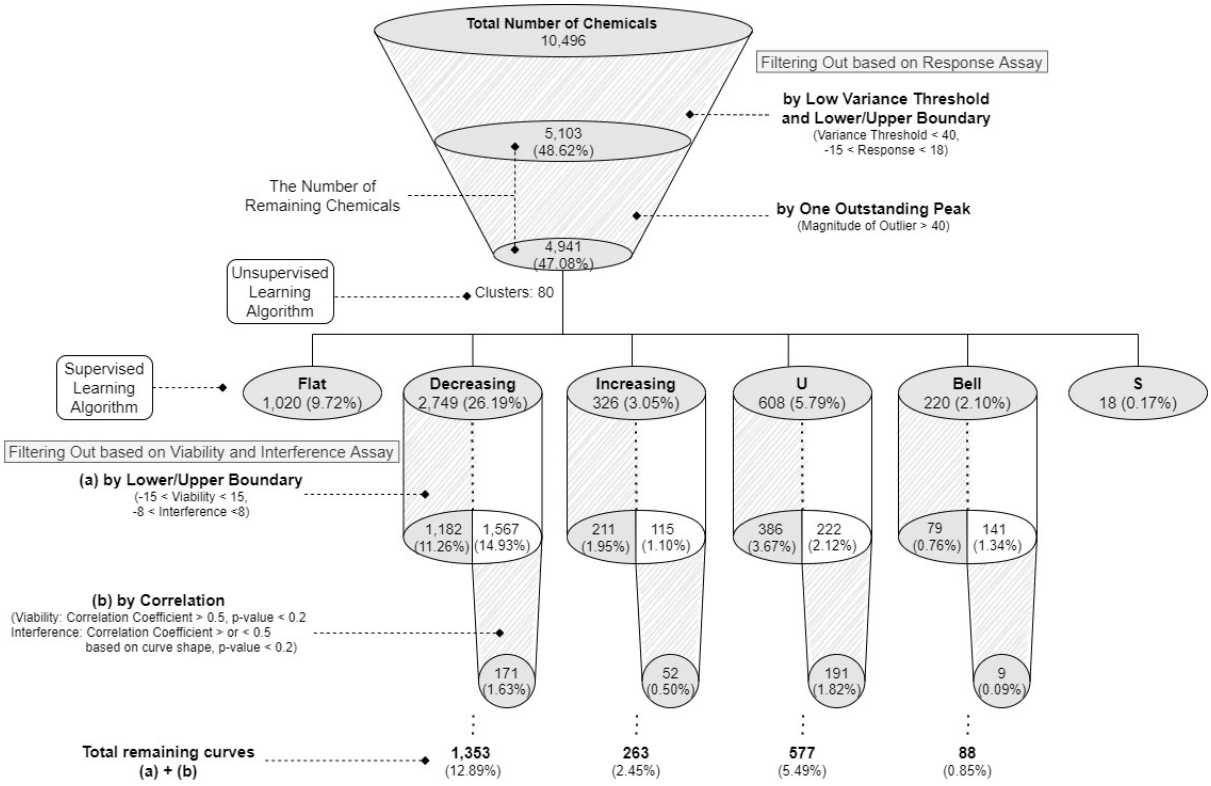

Figure 8. Statistics of concentration-response curves in each shape category after screening (antagonist mode)

3.1.2. Scatter Plots for Lowest Response vs. Highest Response of Monotonically Shaped Curves

Figure 9 is a scatter plot for the distribution of the highest response versus the lowest responses in monotonic decreasing curves showing both cytotoxicity- and interference-screened out and remaining curves. The highest responses are concentrated between -10 and 10, and the lowest

responses are mainly distributed between -140 and 0. Since the baseline responses in TR antagonist mode assay are normalized to zero, most chemicals in decreasing shape start from zero. Figure 9 indicates that a curve's lowest response has nothing to do with where it started (the baseline). Among known TDCs, TBBPA, pentachlorophenol, triclosan, and BPA exhibit as decreasing shapes, however all of them were filtered out through the viability and interference correlation screening steps.

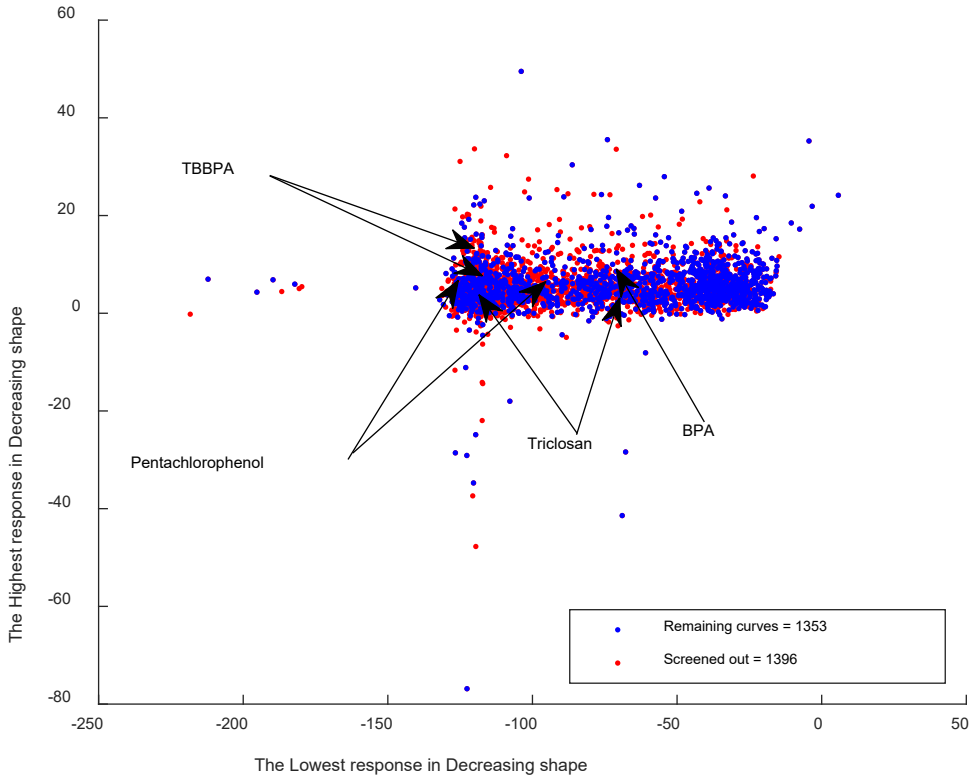

Figure 9. Scatter plot for lowest response vs. highest response of monotonic decreasing curves in TR antagonist assays screened by cytotoxicity and interference assays.

Figure 10 is a scatter plot for the distribution of the highest response versus the lowest responses in monotonic increasing curves for both screened out and remaining curves. This scatter plot shows two clusters. The reason for the existence of the cluster on the left (named cluster A) may be because some curves in that cluster show a sudden drop at a specific concentration point in the middle of the curve, as illustrated in Figure 10-1. All of the curves

in Figure 10-1 are the curves that remain after filtering. Also, there were no known TDCs in the antagonist increasing category.

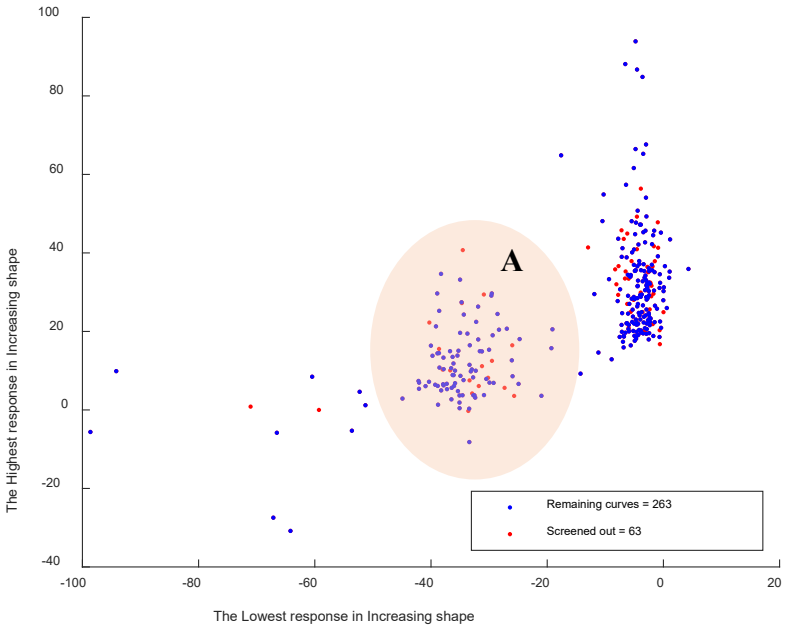

Figure 10. Scatter plot for lowest response vs. highest response of monotonic increasing curves in TR antagonist assays screened by cytotoxicity and interference assays.

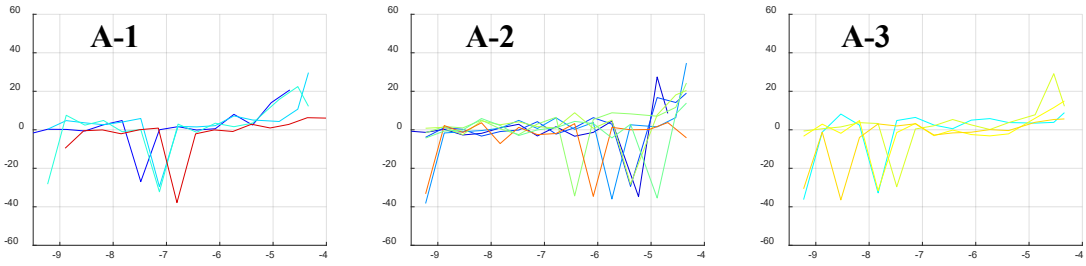

Figure 10-1. Characteristic response curves in cluster A in Figure 10

3.1.3. Scatter Plots for Inflection Point vs. Magnitude in NMDR Curves

Figure 11 presents the $\log_{10}$ inflection-point concentration (M) against NMDR magnitude in the nonmonotonic shapes. It includes 608 U shape curves and 220 Bell shape curves. In both U and Bell categories, $\log_{10}$ inflection-point concentrations were distributed between -9 and -4.5 and the magnitudes were concentrated around 20 regardless of the inflection points. Among

the known TDCs, Methimazole and Propylthiouracil were classified as U shape. There were no known TDCs in the Bell category.

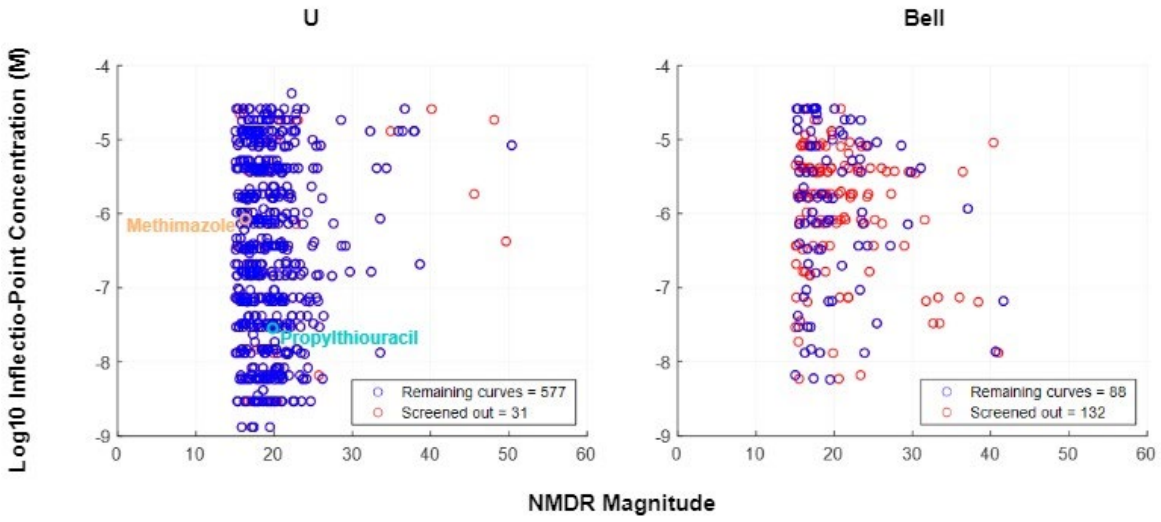

Figure 11. Scatter plots for $\log_{10}$ concentration of inflection point vs. magnitude in U and Bell-shaped curves in the TR antagonist mode assay.

3.1.4. Representative Concentration-Response Curves for Each Category

Representative curves in each category are shown in Figures 12 and 13 where the response curve and the viability curve are presented together. Representative curves in monotonic decreasing shape are fulvestrant (SID 144204490), fluvastatin sodium (SID 144205779), and methysticin (SID 144208099). Representative curves in monotonic increasing shape are rifaximin (SID 144205082), roctopamine hydrochloride (SID 144205777), and decitabine (SID 144205864). Representative curves in U shape are aclarubicin hydrochloride (SID 144206038) and docetaxel (SID 144206639). Representative curves in bell shape are isradipine (SID 144204241) and frentizole (SID 144205517).

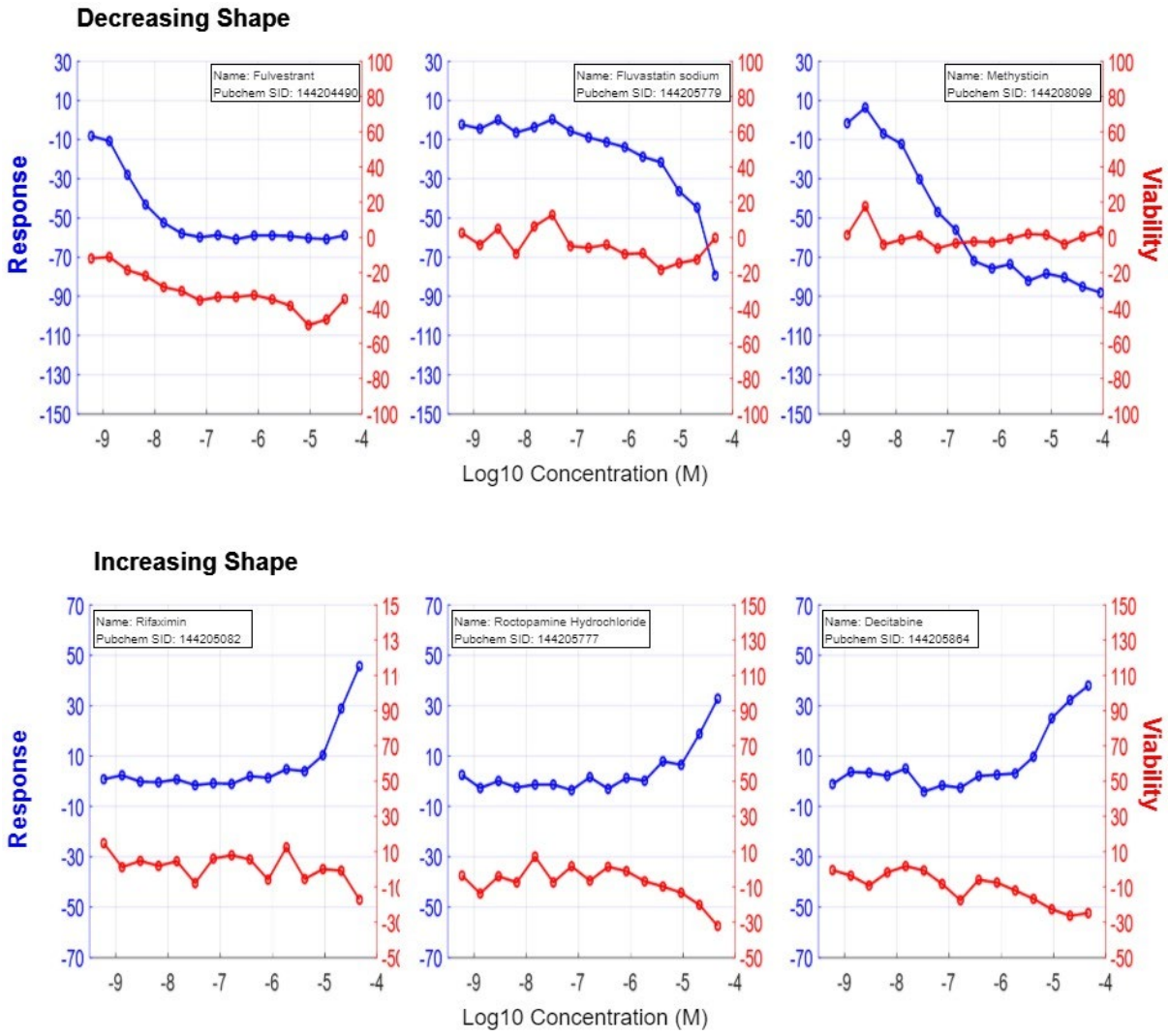

Figure 12. Representative concentration-response curves in monotonic decreasing and increasing shape categories in the TR antagonist mode assay. Blue: response, red: viability.

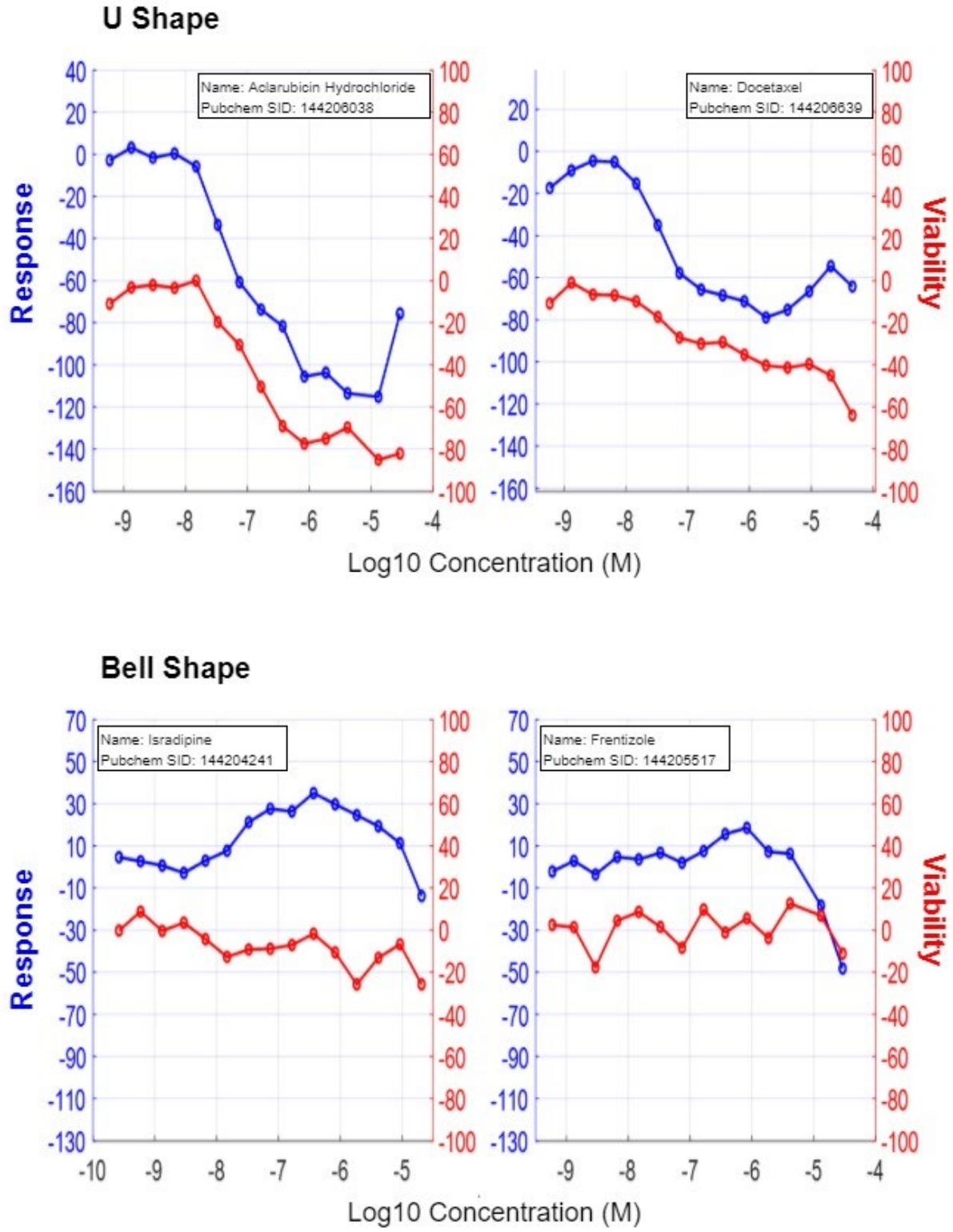

Figure 13. Representative concentration-response curves in nonmonotonic U and Bell shape categories in the TR antagonist mode assay. Blue: response, red: viability.

3.1.5. Hill Coefficient for Monotonic Shapes

The Hill coefficient (curve.n) of the fitted curves are mostly distributed between -5 and 0 except for some extreme cases (Figure 14). Representative fitted curves are shown in Figure 15, including topotecan hydrochloride (curve.n: -4.14), phanquinone (curve.n: -4.19), fenbendzaole (curve.n: -2.08), methylene bis (curve.n: -1.76), and plicamycin (curve.n: -1.73 and -1.76).

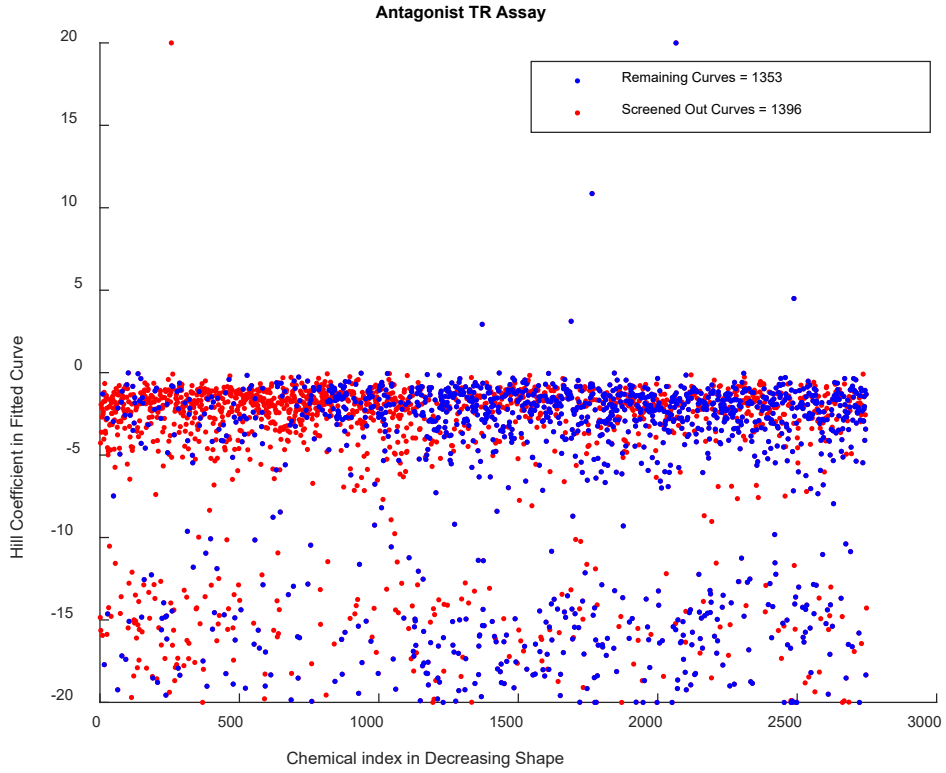

Figure 14. Hill coefficient distribution plot for monotonic decreasing curves in the TR antagonist assay.

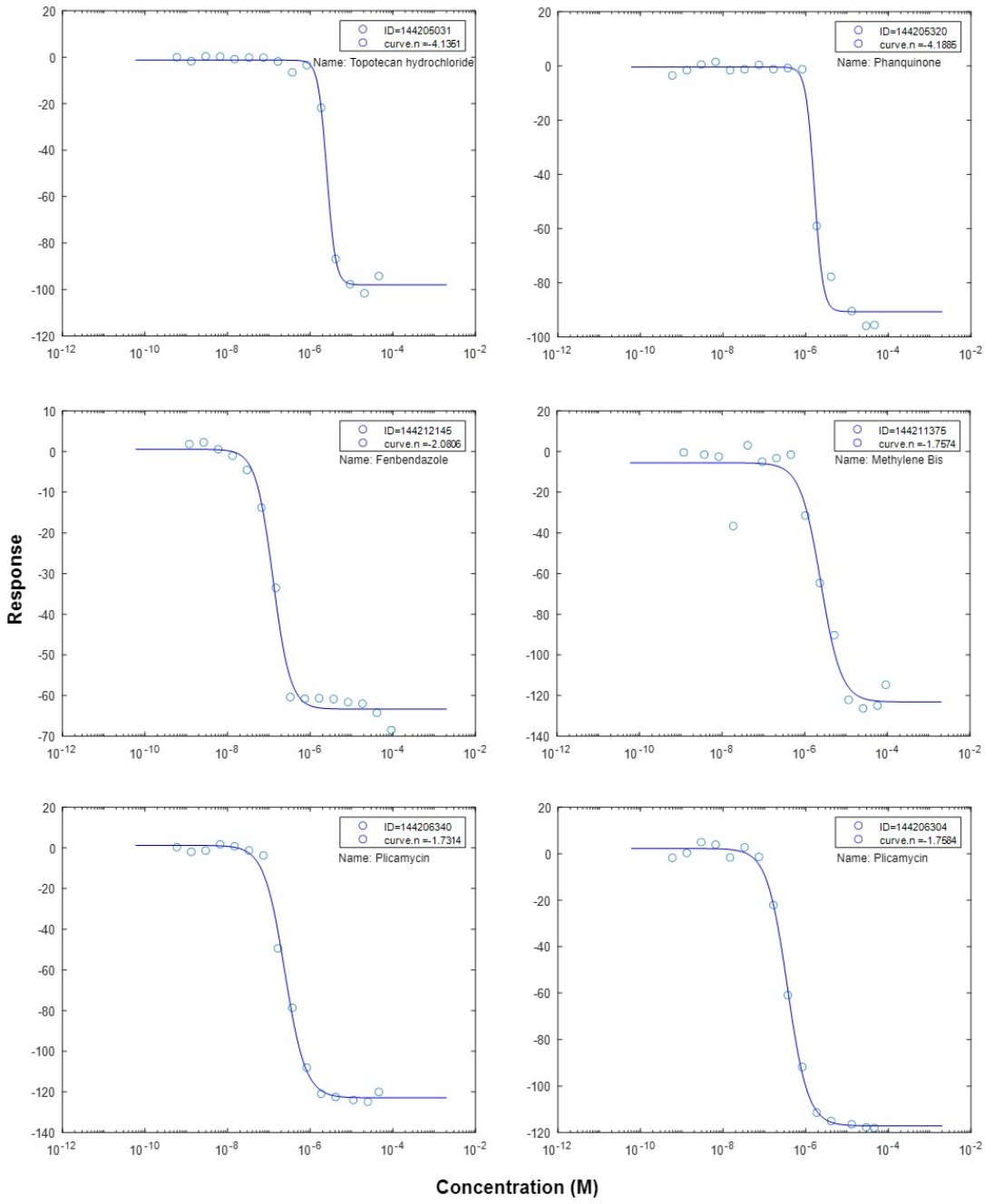

Figure 15. Representative fitted monotonic decreasing curves in the TR antagonist assay.

The Hill coefficients of the monotonic increasing shapes were also obtained, and most of the Hill coefficients values except for few extreme cases were found to be distributed between 0 and 20 (figure 16). Representative fitted curves were shown in Figure 17 including naproxol (curve.n: 3.21), rifaximin (curve.n: 1.65), decitabine (curve.n: 1.92), and sodium 2-mercaptobenzothiolate (curve.n: 3.57).

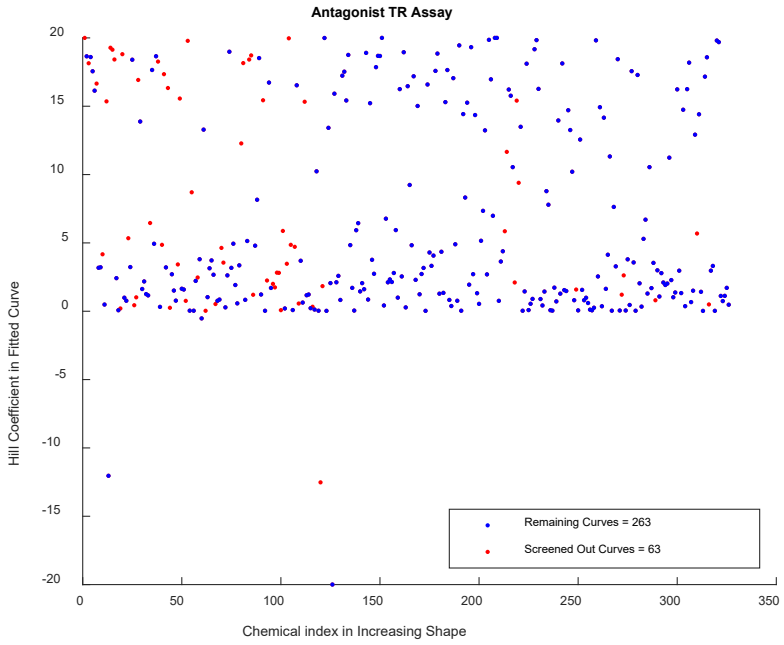

Figure 16. Hill coefficient distribution plot for monotonic increasing curves in the TR antagonist assay.

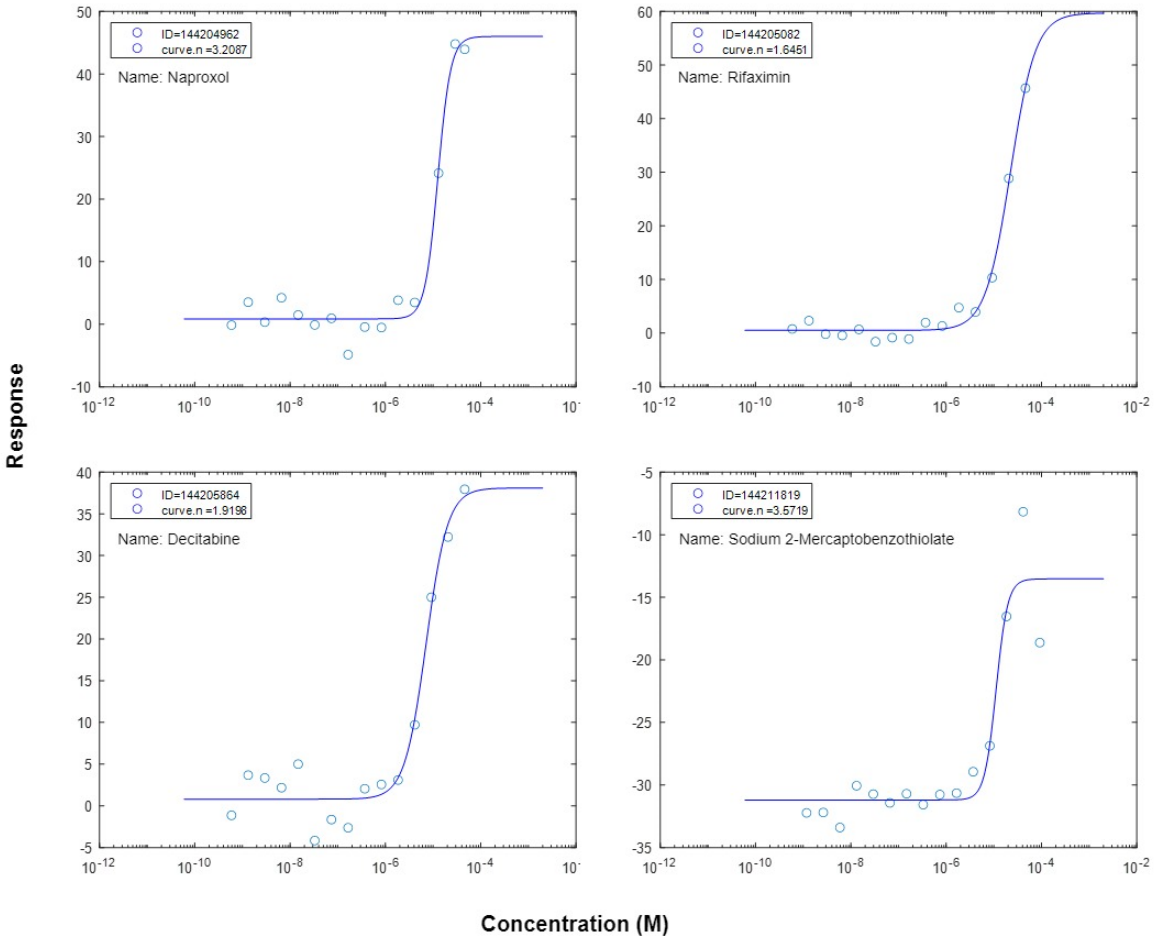

Figure 17. Representative fitted monotonic increasing curves in the TR antagonist assay.

3.2. Agonist Assay Results

3.2.1. Statistics of Concentration-Response Curves in Each Shape

Screening was conducted twice on response data in TR agonist mode assay (Figure 18). Through the first screening criteria, 10,418 of all chemicals were filtered, leaving 78 (0.74%) of chemicals. No chemicals were excluded through the second screening criterion, before applying the unsupervised and supervised learning algorithm.

As a result of applying the unsupervised algorithm, where the correlation of the chemical dose-response curves is 0.75 or higher, a total of 8 clusters were formed. These clusters were visually inspected and were consolidated into 5 categories: flat, monotonic decreasing, monotonic increasing, U, and Bell curves. After applying the supervised algorithm, the curves were classified into 33 flat curves (0.31%), 16 decreasing curves (0.15%), 19 increasing curves (0.18%), 1 U curve (0.01%), and 9 Bell curves (0.09%).

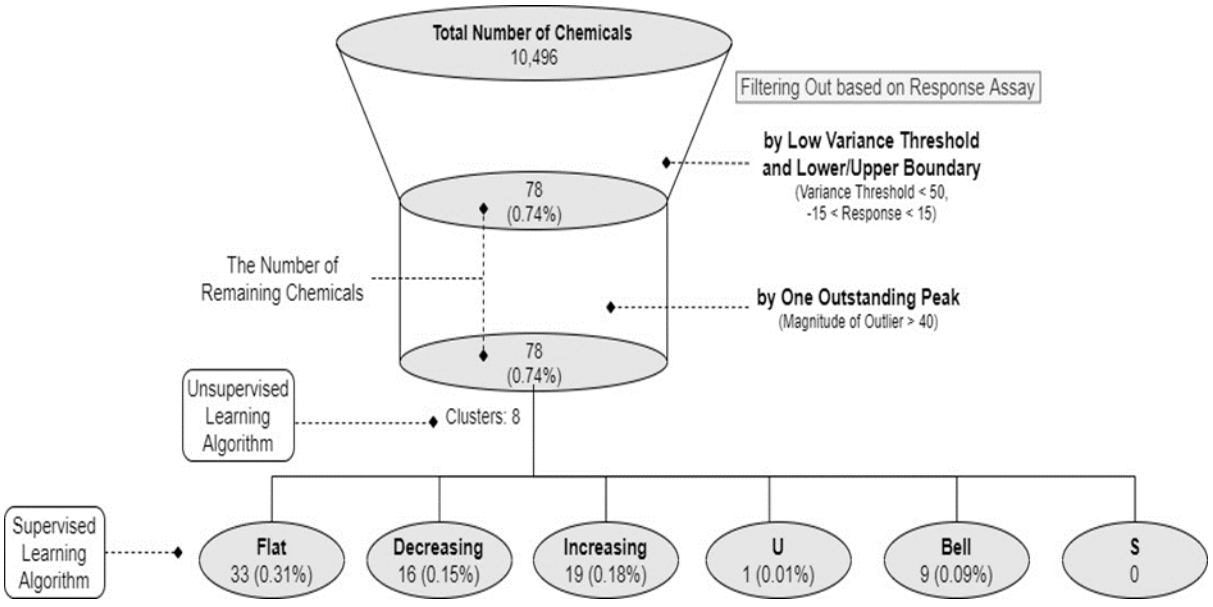

Figure 18. Statistics of curves in each shape in the TR agonist mode assay

3.2.2. Scatter Plots for Lowest Response vs. Highest Response in Each Monotonic Shape

Figure 19 is a scatter plot for the distribution of the highest response versus the lowest responses in decreasing shape curves in agonist mode assay. The starting points (the highest responses) of chemicals classified as agonist decreasing shape were distributed from 10 up to over 100. The highest response and the lowest response appear to have a positive correlation. There were no known TDCs in the agonist decreasing category.

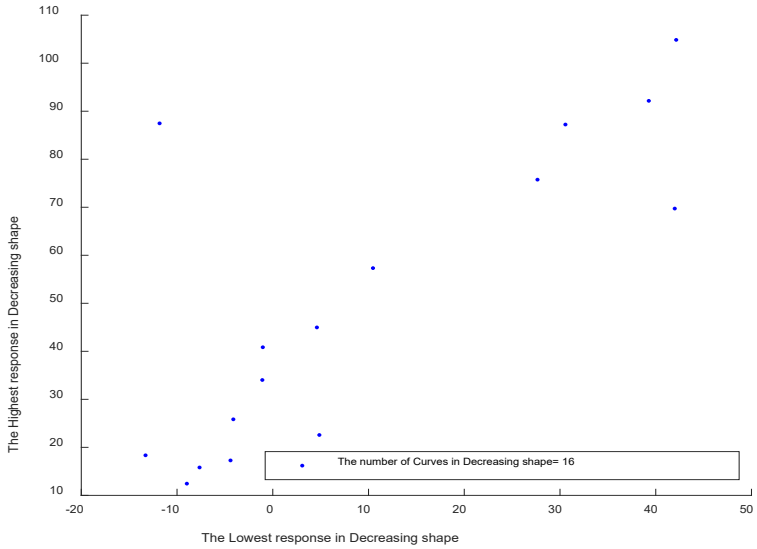

Figure 19. Scatter plot for lowest response vs. highest response of monotonic decreasing curves in TR agonist assays.

Figure 20 is a scatter plot for the distribution of the highest response versus the lowest responses in increasing shape curves in agonist mode assay. The concentration-response curves mostly start at 0 and have different highest responses at around 20-100. As in the antagonist decreasing assay, the low starting point and the highest response value were not correlated with each other. There were no known TDCs in the agonist increasing category.

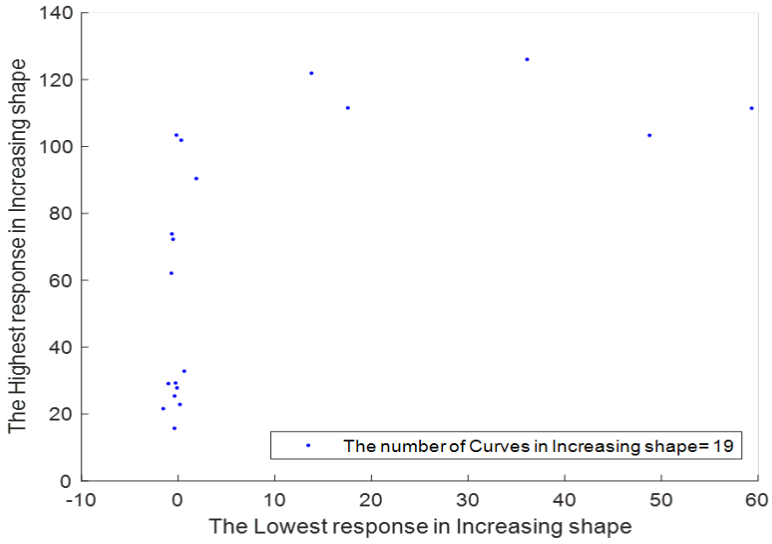

Figure 20. Scatter plot for lowest response vs. highest response of monotonic increasing curves in TR agonist assays.

3.2.3. Scatter Plots for Inflection Point vs. Magnitude in NMDR curves

Figure 21 presents $\log_{10}$ inflection-point concentration (M) against NMDR magnitude in agonist nonmonotonic shapes, including all of the nonmonotonic curves (1 U shape curve, 9 Bell shape curves, respectively). In both U and Bell categories, $\log_{10}$ inflection-point concentrations were distributed between -7 and -5, and the magnitudes were around 20, which was similar to the findings in antagonist mode scatter plot (Figure 11). There were no known TDCs in nonmonotonic categories.

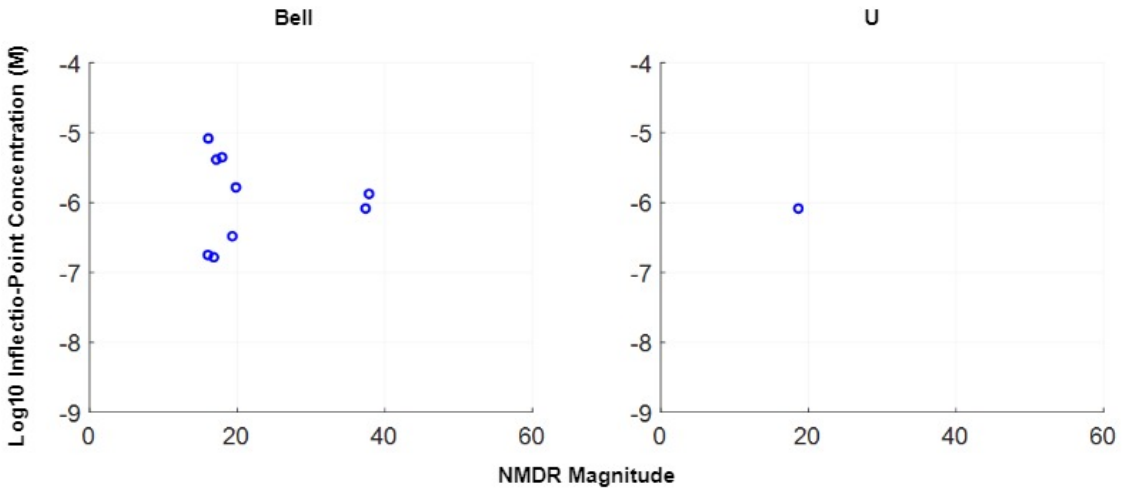

Figure 21. Scatter plots for $\log_{10}$ concentration of inflection point vs. magnitude in U and Bell shaped curves in TR agonist mode assays.

3.2.4. Representative Curves for Each Category

Representative curves in each category are shown in Figures 22 and 23 where the response curve and the viability curve are presented together. Representative curves in decreasing shape are methylcarbamycholine chloride (SID 144204809), (7S)-hydroprene (SID 144205353), and epsilon-decalactone (SID 144212779). Representative curves in increasing shape are levothyroxine (SID 144205654), 2'.3'-dideoxyinosine (SID 144209531), and equilin (SID 144212958). Representative curve in U shape is cresol (SID 144206791). Representative curves in bell shape are all-trans-retinoic acid (SID 144210625) and bexarotene (SID 144212724).

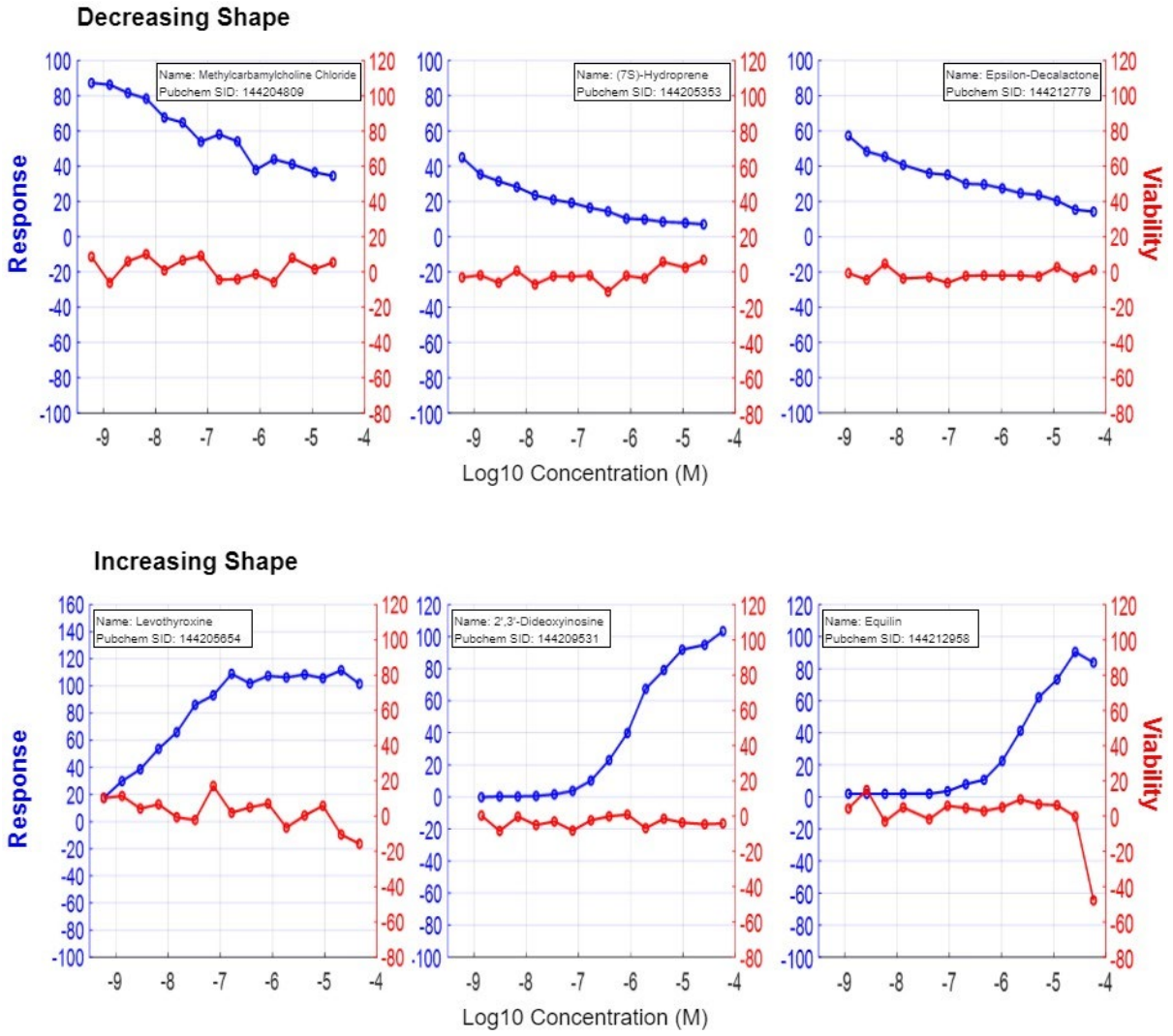

Figure 12. Representative curves in monotonic decreasing and increasing shape categories in the TR agonist assay. Blue: response, red: viability.

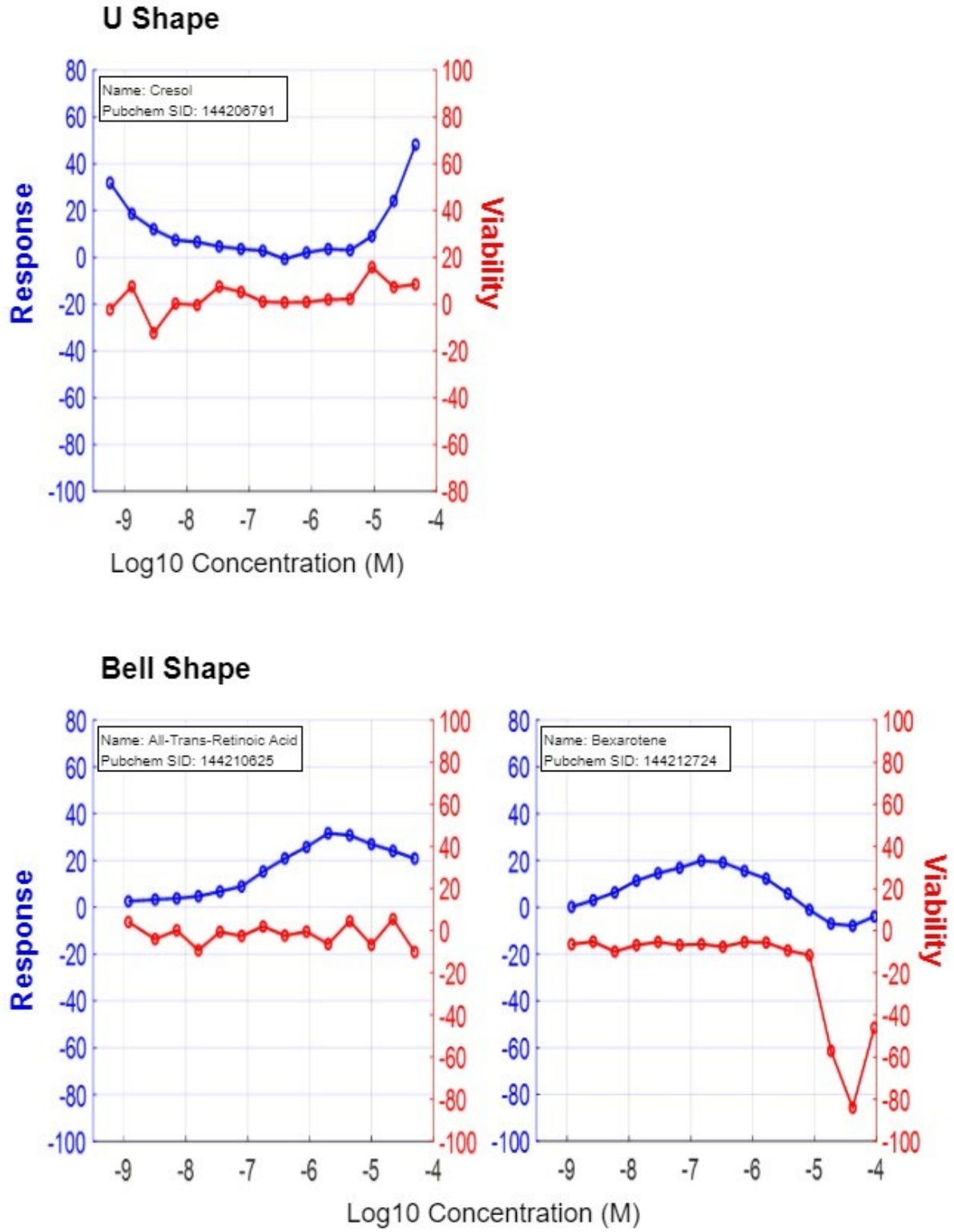

Figure 23. Representative curves in nonmonotonic U and Bell shape categories in the TR agonist assay. Blue: response, red: viability.

3.2.5. Hill Coefficient for Monotonic Shapes

The hill coefficient (curve.n) of the fitted curves are mostly distributed between -2 and 0 (Figure 24). Representatively fitted curves (Figure 25) were triphenyltin hydroxide (curve.n: -1.69) and triphenyltin acetate (curve.n: -1.75).

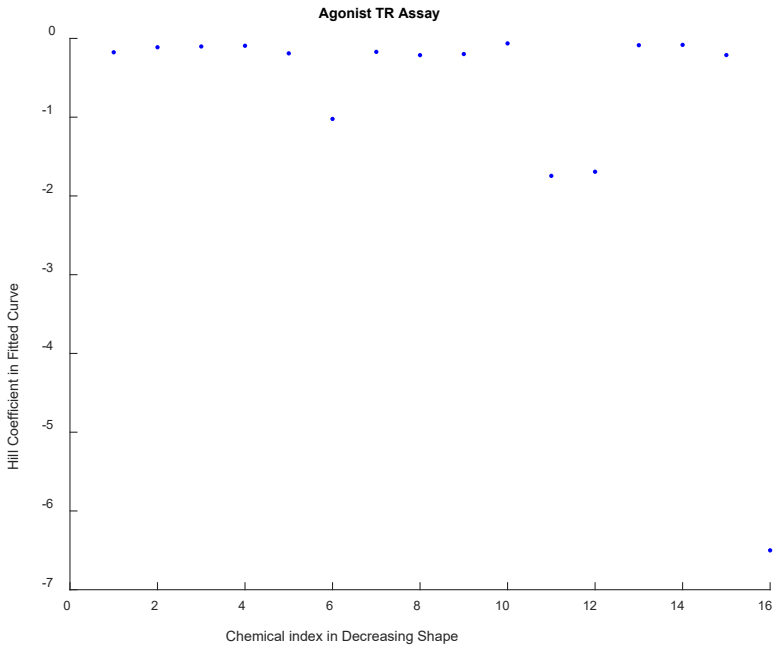

Figure 24. Hill coefficient distribution plot for monotonic decreasing curves in the TR agonist assay.

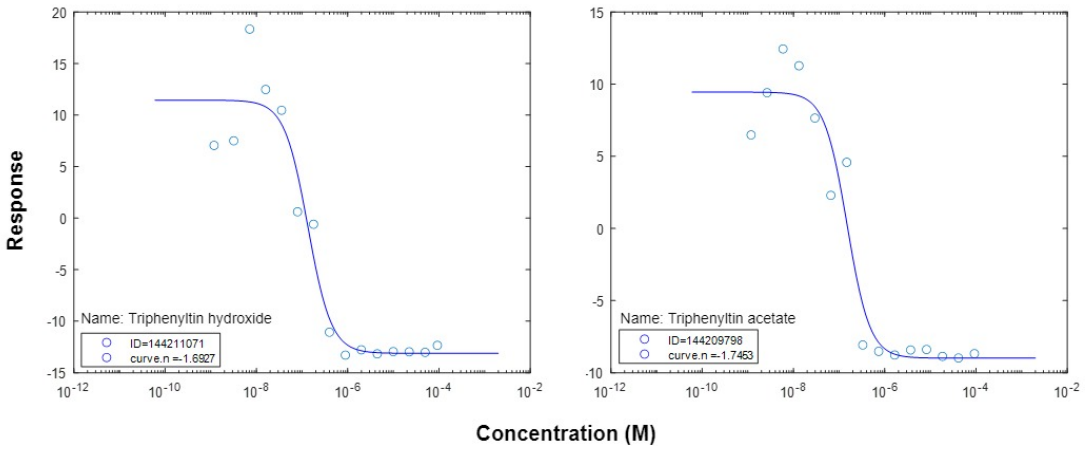

Figure 25. Representative fitted monotonic decreasing curves in the TR agonist assay.

The Hill coefficients of the increasing shapes were also obtained and most of the Hill coefficients values excluding few outliers were found to be distributed around 1-2 (Figure 26). Representatively fitted curves (Figure 27) were, 3,3'5'-triiodo-L-thyronine (curve.n: 1.02), 2',3'-dideoxyinosine (curve.n: 1.09), levothyroxine (curve.n: 1.74), and equilin (curve.n: 2.08).

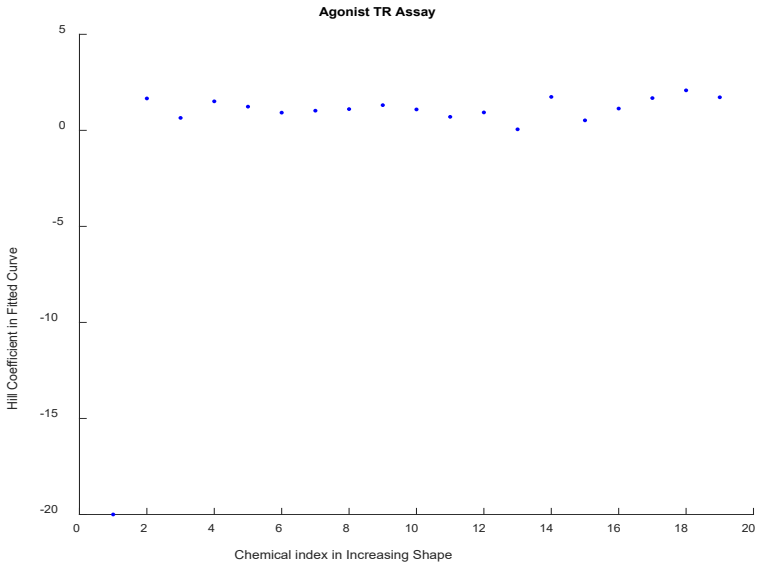

Figure 26. Hill coefficient distribution plot for monotonic increasing curves in the TR agonist assay.

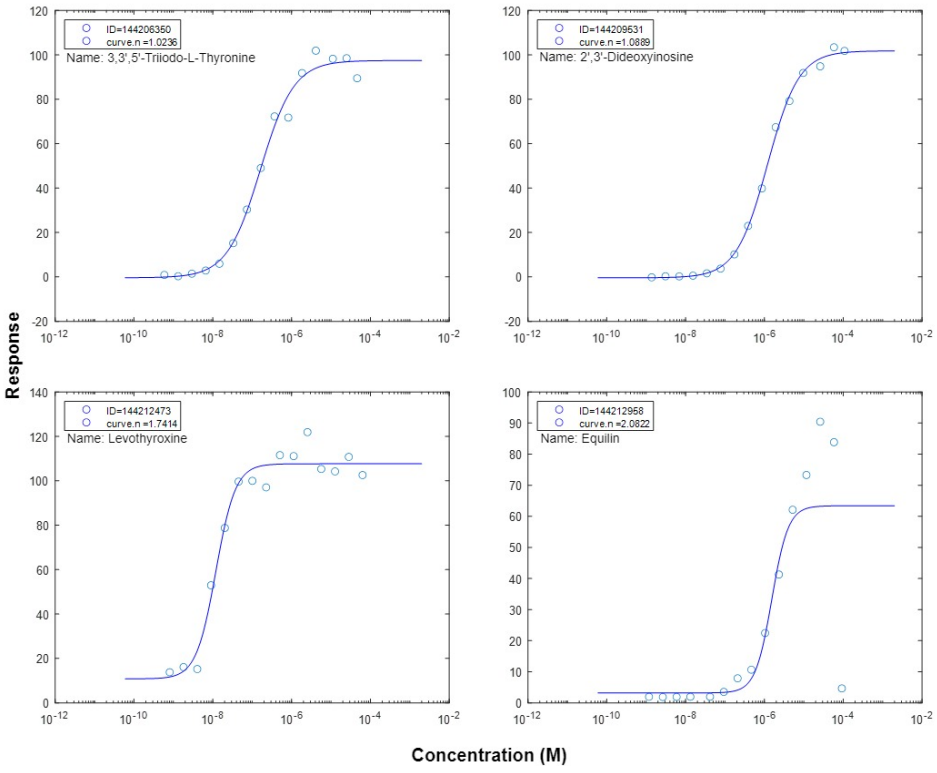

Figure 27. Representative fitted monotonic increasing curves in the TR agonist assay.

3.3. Comparison between Agonist and Antagonist Assay Results

Figure 28 shows the maximum/minimum response comparison between antagonist analysis and agonist analysis for 10K chemicals, divided into 4 combinations. Figure 28B shows that minimal responses in both assays appear to have positive correlation, which means the smaller the minimum value of agonist in one chemical, the stronger the response of the antagonist response occurs. Figure 28D shows that there are much fewer positive responses for the agonist assay than for antagonist assay. Chemicals that have positive responses in both assays are highlighted in the shaded zone in Figure 28D, and less than 10 are observed. These include 3,5,3'-Triiodothyronine, ecopipam, 3,3',5'-triiodo-L-thyronine, equilin, tetrac, and tiratricol. Figure 28-1 shows simultaneously the antagonist, agonist, viability, and interference concentration-response curves of these chemicals.

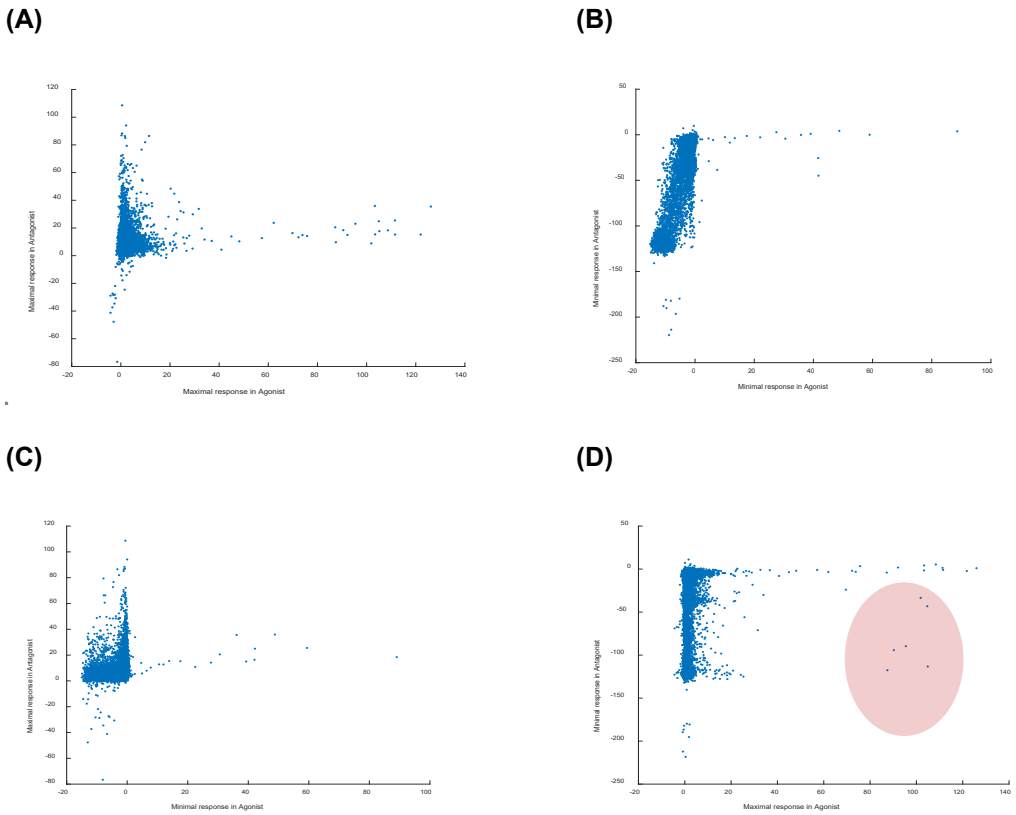

Figure 28. Maximum/minimum response comparisons between TR antagonist and agonist assays

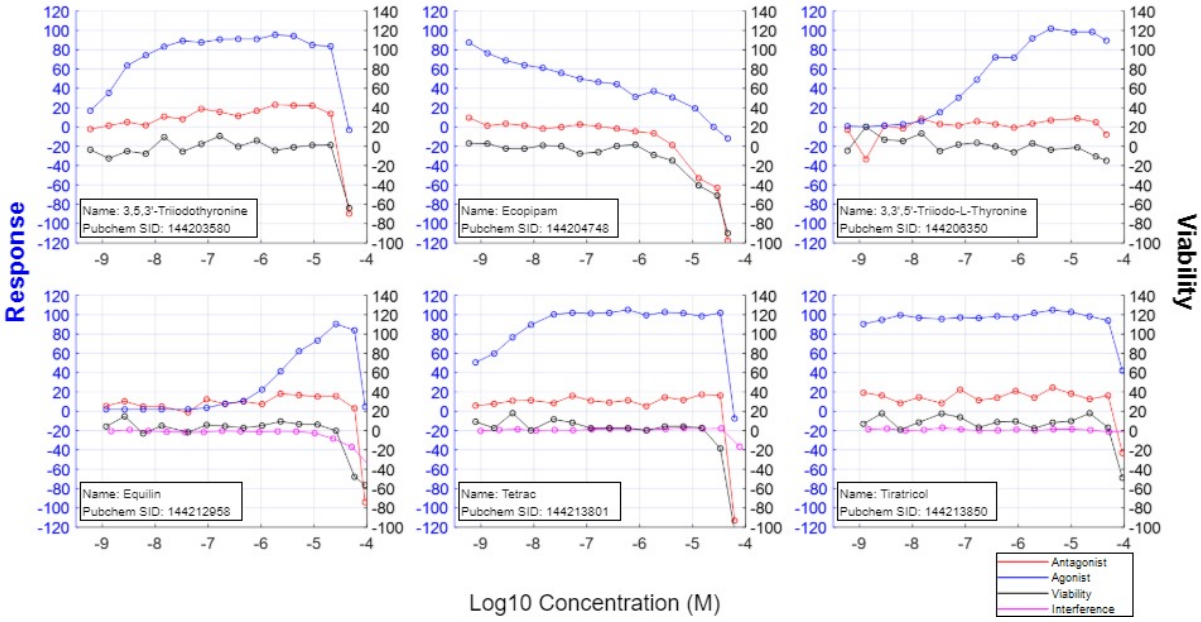

Figure 28-1. Concentration-response curves with both positive response to antagonist and agonist

4. Discussion

4.1. Linking to the Literatures

This study identified and analyzed TR NMDR and other nonlinear relationships in publicly available Tox21 TR assays based on a custom-developed learning algorithm. After initial screening to exclude those chemicals that exhibit no activity in agonist or antagonist mode, the respective concentration-response curves were divided into five to six shapes. False-positive results were further filtered by utilizing two types of assays, viability, and interference (luciferase) assays. The chemicals belonging to the U and Bell shapes were identified as NMDR pattern. For the monotonic shapes, the Hill function was applied to assess their nonlinearities.

Among the various chemicals mentioned as known TDCs in Miller, Crofton et al. (2009), methimazole, benzophenone-2, and PTU in antagonist mode assay showed NMDR relationships. Other chemicals referred to as TDCs in Miller, Crofton et al. (2009) were triclosan, BPA, TBBPA, acetochlor, and pentachlorophenol, most of which were classified as monotonic decreasing curves, i.e., they function as an antagonist. Although the above chemicals were classified as monotonic curves, the Hill coefficients ranged from -14.28 to -1.63 (except for TBBPAs ranged from -1.33 to -0.98), which represent considerably high nonlinearities given that most of the Hill coefficients in the monotonic decreasing curves were distributed between -5 and 0. These chemicals, classified either as nonmonotonic or monotonic, but with relatively high nonlinearities, are in line with the characteristics of EDCs in that their concentration-response relationships can be complex. For the agonist mode assay, none of the known TDC chemicals were identified in any categories of the response curves. It is interesting to note that there are so fewer positive responses for agonist assay than for antagonist assay. When comparing the maximum responses as an agonist, and the minimum responses as an

antagonist, the maximum response was very small compared to the minimal response (Figure 28). This result suggests that among the 10K library of chemicals tested, many chemicals can compete with T_3 for TR, however, their binding with TR does not initiate the classical TR-mediated signaling through TREs. Rather, they may just function as either passive or active repressors antagonizing the action of T_3.

Numerous theories have been hypothesized about the biological mechanisms of NMDR behaviors, which include i) opposing biological actions via two nuclear receptor isoforms, ii) nuclear receptor homodimerization, iii) formation of mixed-ligand receptor heterodimers, iv) weak coactivator recruitment by EDC-liganded spare receptors on promotors, v) incoherent feedforward through membrane and nuclear receptors, vi) ligand-induced receptor desensitization or degradation, vii) opposing effects of parent compound and its metabolite, viii) coactivator squelching, ix) induction of repressor, and x) negative feedback (Kohn and Portier 1993, Kohn and Melnick 2002, Conolly and Lutz 2004, Li, Andersen et al. 2007, Vandenberg, Colborn et al. 2012, Cookman and Belcher 2014, Lagarde, Beausoleil et al. 2015, Xu, Liu et al. 2017). While most of the mechanisms listed above remain to be validated, several computational models have been studied to investigate NMDR mechanisms within the classical nuclear receptor-mediated endocrine signaling framework (Kohn and Portier 1993, Kohn and Melnick 2002, Conolly and Lutz 2004, Li, Andersen et al. 2007). It is likely that the NMDR observed in the Tox21 TR assays may result from some of these mechanisms, which require further experiments to confirm.

4.2. Pros. and Cons. of the Study

The methodology of our study has the following limitations. Firstly, only the luciferase inhibition assay was used in the interference screening process. Autofluorescence assay was

not included to screen for positive results in the viability assays that may be due to autofluorescence. Secondly, the NMDR relationships discovered *in vitro* do not necessarily occur in vivo. Thirdly, beyond NMDR identification using the machine learning algorithms, modeling these responses to give a deeper understanding of the in-depth molecular mechanisms will need to be conducted in the future.

Although there are limitations as described above, our study has the following strengths. Firstly, through the use of learning algorithms, it is able to analyze 10K chemicals and identify hundreds of chemicals with NMDR patterns in TR antagonist and agonist assays. Secondly, for the same chemical, the unique concentration-response data profiles in both agonist and antagonist mode provide a cornerstone for understanding the NMDR mechanism in TR assays. Thirdly, the custom-developed learning algorithms for TR NMDR identification are well suited for exploring other nuclear receptor high-throughput Tox21 assays as well.

4.3. In relationship to other TH related assay results

In our study, we looked at the TR signaling pathway as one of the factors that can be altered by TH levels in circulation. In order to better understand the impact on human health due to changes in TH levels, it is also necessary to evaluate whether EDCs can disrupt thyroid function at the thyroid stimulating hormone receptor (TSHR) and thyrotropin-releasing hormone receptor (TRHR) levels.

Shobair, Nelms et al. (2019) conducted a study to identify antagonists and agonists that can disrupt the TSHR signaling pathway. Of the 7,872 tested chemicals in this study, 441 agonists (6%), 287 antagonists (4%), and 49 (0.6%) agonists and simultaneously antagonists were identified. Because receptor binding is specific and selective, they hypothesized in the

study that a large number of chemical results would be false positives. Accordingly, after conducting assays on autofluorescence and cytotoxicity, the result was that cytotoxicity had a significant effect on the antagonist priority rank as 68% of antagonists were found to be due to cytotoxicity. They suggested that phenols, organochlorine insecticides, and retinoids belong to agonist clusters. Shobair (2020) attempted integrating data in silico and in vitro to identify TRHR ligands. They identified 71 agonists (1%), 160 antagonists (2.1%), and 157 (2%) as both agonists and antagonists out of 7,872 tested chemicals, however, false negatives and positives cannot be ruled out without additional screening assays. Therefore, the main area going forward should be focused on how false positives and false negatives can be better screened out in studies related to TH assays.

5. Conclusion

It should be admitted that our current understanding of how exposure at various concentrations of numerous endocrine disruptors, including TDCs, will ultimately affect the human body is extremely fragmented and limited. Nevertheless, beyond the traditional research techniques currently used in most exposure risk assessment fields, mathematical modeling techniques in systems biology and new research techniques including machine learning have been expanding their territories to evaluate the health effects of endocrine disruptors (Soto and Sonnenschein 2010). The customized MATLAB algorithms we used here help us to better understand nonlinear relationships of environmental exposures. The nonlinearity in the response of a chemical has important implications in accurately predicting the risk of exposure to the chemical. Therefore, identifying nonlinear concentration-response relationship will help provide a scientific basis for improving safety assessment of chemical products that humans are exposed to in daily life.

References

Bernal, J. (2005). "Thyroid hormones and brain development." Vitam Horm **71**: 95-122.

Boas, M., U. Feldt-Rasmussen and K. M. Main (2012). "Thyroid effects of endocrine disrupting chemicals." Mol Cell Endocrinol **355**(2): 240-248.

Boas, M., U. Feldt-Rasmussen, N. E. Skakkebaek and K. M. Main (2006). "Environmental chemicals and thyroid function." Eur J Endocrinol **154**(5): 599-611.

Cargnelutti, F., A. Di Nisio, F. Pallotti, I. Sabovic, M. Spaziani, M. G. Tarsitano, D. Paoli and C. Foresta (2020). "Effects of endocrine disruptors on fetal testis development, male puberty, and transition age." Endocrine.

Conolly, R. B. and W. K. Lutz (2004). "Nonmonotonic dose-response relationships: mechanistic basis, kinetic modeling, and implications for risk assessment." Toxicol Sci **77**(1): 151-157.

Cookman, C. J. and S. M. Belcher (2014). "Classical nuclear hormone receptor activity as a mediator of complex concentration response relationships for endocrine active compounds." Curr Opin Pharmacol **19**: 112-119.

Cote, I., P. T. Anastas, L. S. Birnbaum, R. M. Clark, D. J. Dix, S. W. Edwards and P. W. Preuss (2012). "Advancing the next generation of health risk assessment." Environ Health Perspect **120**(11): 1499-1502.

Crofton, K. M. and R. T. Zoeller (2005). "Mode of action: neurotoxicity induced by thyroid hormone disruption during development--hearing loss resulting from exposure to PHAHs." Crit Rev Toxicol **35**(8-9): 757-769.

Dix, D. J., K. A. Houck, M. T. Martin, A. M. Richard, R. W. Setzer and R. J. Kavlock (2007). "The ToxCast program for prioritizing toxicity testing of environmental chemicals." Toxicol Sci **95**(1): 5-12.

Fliers, E., A. Kalsbeek and A. Boelen (2014). "Beyond the fixed setpoint of the hypothalamus-pituitary-thyroid axis." Eur J Endocrinol **171**(5): R197-208.

Freitas, J. (2012). "Development and Validation of *in vitro* Bioassays for Thyroid Hormone Receptor mediated Endocrine Disruption."

Freitas, J., N. Miller, B. J. Mengeling, M. Xia, R. Huang, K. Houck, I. M. Rietjens, J. D. Furlow and A. J. Murk (2014). "Identification of thyroid hormone receptor active compounds using a quantitative high-throughput screening platform." Curr Chem Genom Transl Med **8**: 36-46.

Ghisari, M. and E. C. Bonefeld-Jorgensen (2005). "Impact of environmental chemicals on the thyroid hormone function in pituitary rat GH3 cells." Mol Cell Endocrinol **244**(1-2): 31-41.

Ghisari, M. and E. C. Bonefeld-Jorgensen (2009). "Effects of plasticizers and their mixtures on estrogen receptor and thyroid hormone functions." Toxicol Lett **189**(1): 67-77.

Grimaldi, M., A. Boulahtouf, V. Delfosse, E. Thouennon, W. Bourguet and P. Balaguer (2015). "Reporter Cell Lines for the Characterization of the Interactions between Human Nuclear Receptors and Endocrine Disruptors." Front Endocrinol (Lausanne) **6**: 62.

Howdeshell, K. L. (2002). "A model of the development of the brain as a construct of the thyroid system." Environ Health Perspect **110 Suppl 3**: 337-348.

Hsieh, J. H., A. Sedykh, R. Huang, M. Xia and R. R. Tice (2015). "A Data Analysis Pipeline Accounting for Artifacts in Tox21 Quantitative High-Throughput Screening Assays." J Biomol Screen **20**(7): 887-897.

Klimenko, K. (2021). "Examining the evidence of non-monotonic dose-response in Androgen Receptor agonism high-throughput screening assay." Toxicol Appl Pharmacol **410**: 115338.

Kohn, M. C. and R. L. Melnick (2002). "Biochemical origins of the non-monotonic receptor-mediated dose-response." J Mol Endocrinol **29**(1): 113-123.

Kohn, M. C. and C. J. Portier (1993). "Effects of the mechanism of receptor-mediated gene expression on the shape of the dose-response curve." Risk Anal **13**(5): 565-572.

Krewski, D., M. Westphal, M. E. Andersen, G. M. Paoli, W. A. Chiu, M. Al-Zoughool, M. C. Croteau, L. D. Burgoon and I. Cote (2014). "A framework for the next generation of risk science." Environ Health Perspect **122**(8): 796-805.

Lagarde, F., C. Beausoleil, S. M. Belcher, L. P. Belzunces, C. Emond, M. Guerbet and C. Rousselle (2015). "Non-monotonic dose-response relationships and endocrine disruptors: a qualitative method of assessment." Environ Health **14**: 13.

Li, L., M. E. Andersen, S. Heber and Q. Zhang (2007). "Non-monotonic dose-response relationship in steroid hormone receptor-mediated gene expression." J Mol Endocrinol **38**(5): 569-585.

Medici, M., W. E. Visser, T. J. Visser and R. P. Peeters (2015). "Genetic determination of the hypothalamic-pituitary-thyroid axis: where do we stand?" Endocr Rev **36**(2): 214-244.

Meeker, J. D., L. Altshul and R. Hauser (2007). "Serum PCBs, p,p'-DDE and HCB predict thyroid hormone levels in men." Environ Res **104**(2): 296-304.

Miller, M. D., K. M. Crofton, D. C. Rice and R. T. Zoeller (2009). "Thyroid-disrupting chemicals: interpreting upstream biomarkers of adverse outcomes." Environ Health Perspect **117**(7): 1033-1041.

Miller, M. M., P. D. McMullen, M. E. Andersen and R. A. Clewell (2017). "Multiple receptors shape the estrogen response pathway and are critical considerations for the future of in vitro-based risk assessment efforts." Crit Rev Toxicol **47**(7): 564-580.

Morreale de Escobar, G., M. J. Obregon and F. Escobar del Rey (2004). "Role of thyroid hormone during early brain development." Eur J Endocrinol **151 Suppl 3**: U25-37.

Schug, T. T., A. Janesick, B. Blumberg and J. J. Heindel (2011). "Endocrine disrupting chemicals and disease susceptibility." J Steroid Biochem Mol Biol **127**(3-5): 204-215.

Shi, Z., M. Xia and Q. Zhang (2020). "Computational Identification and Analysis of Nonmonotonic Concentration Responses in Tox21 Estrogen Receptor Assays."

Shobair, M. (2020). Integrating *in silico* and *in vitro* data to identify putative thyrotropin-releasing hormone receptor ligands.

Shobair, M., M. Nelms, C. Deisenroth, G. Patlewicz and K. Paul-Friedman (2019). A high-throughput approach to identify and prioritize putative thyroid-stimulating hormone receptor agonists and antagonists.

Silva, J. E. (2001). "The multiple contributions of thyroid hormone to heat production." J Clin Invest **108**(1): 35-37.

Soto, A. M. and C. Sonnenschein (2010). "Environmental causes of cancer: endocrine disruptors as carcinogens." Nat Rev Endocrinol **6**(7): 363-370.

Vandenberg, L. N., T. Colborn, T. B. Hayes, J. J. Heindel, D. R. Jacobs, Jr., D. H. Lee, T. Shioda, A. M. Soto, F. S. vom Saal, W. V. Welshons, R. T. Zoeller and J. P. Myers (2012). "Hormones and endocrine-disrupting chemicals: low-dose effects and nonmonotonic dose responses." Endocr Rev **33**(3): 378-455.

Xu, Z., J. Liu, X. Wu, B. Huang and X. Pan (2017). "Nonmonotonic responses to low doses of xenoestrogens: A review." Environ Res **155**: 199-207.

Yen, P. M. (2001). "Physiological and molecular basis of thyroid hormone action." Physiol Rev **81**(3): 1097-1142.

Zhang, Q., J. Li, A. Middleton, S. Bhattacharya and R. B. Conolly (2018). "Bridging the Data Gap From in vitro Toxicity Testing to Chemical Safety Assessment Through Computational Modeling." Front Public Health **6**: 261.

Zoeller, R. T., S. W. Tan and R. W. Tyl (2007). "General background on the hypothalamic-pituitary-thyroid (HPT) axis." Crit Rev Toxicol **37**(1-2): 11-53.